Pressure
Sciences
Incorporated
Towne Centre Offices, Suite 290
1789 South Braddock Avenue
Pittsburgh, PA 15218-1868
(412) 371-3117 Fax (412) 371-0424

Improving Crashworthiness of Front Heads of MC-331 Cargo Tank Motor Vehicles

Allen Selz, Ph.D., P.E., and Clayton F. Heberling, P.E.

Report No. 98025-007
February 2000

Prepared for
U.S. Department of Transportation
Research and Special Programs Administration
400 Seventh St., SW, Washington, D.C. 20590

under Requisition No. 957-6228
Order No. DTRS56-98-P-70073

REPORT DOCUMENTATION PAGE

Form Approved
OMB No. 0704-0188

1. AGENCY USE ONLY *(Leave blank)*	2. REPORT DATE	3. REPORT TYPE AND DATES COVERED
	February 2000	Final Report

4. TITLE AND SUBTITLE
Improving Crashworthiness of Front Head of MC-331 Cargo Tank Motor Vehicles

5. FUNDING NUMBERS
Order No. DTRS 56-98-P-70073

6. AUTHORS
Allen Selz, Ph.D., P.E. and Clayton F. Heberling, P.E.

7. PERFORMING ORGANIZATION NAME(S) AND ADDRESS(ES)
Pressure Sciences Incorporated
1789 S. Braddock Ave. Ste. 290
Pittsburgh PA 15218

8. PERFORMING ORGANIZATION REPORT NUMBER
98025-007

9. SPONSORING/MONITORING AGENCY NAME(S) AND ADDRESS(ES)
U.S. Department of Transportation - COTR - Ronald Kirkpatrick
Research and Special Projects Administration
Office of Contracts and Procurement (DMA-30)
400 Seventh Street, S.W., Room 8321, Washington, D.C. 20590

10. SPONSORING/MONITORING AGENCY REPORT NUMBER

11. SUPPLEMENTARY NOTES

12a. DISTRIBUTION/AVAILABILITY STATEMENT	12b. DISTRIBUTION CODE

13. ABSTRACT *(Maximum 200 words)*

Analyses using ANSYS and LS-DYNA were performed to determine the response of MC-331 pressurized cargo tank heads when striking various obstacles. The incorporation of head shielding was shown to improve the crashworthiness for angled impacts into a wall or impact with a bridge support column. Only minor protection against normal (perpendicular) impacts into a rigid flat surface or rigid post is a realistic goal. Correlations to an accident that occurred in White Plains, NY were used to validate the finite element model. Additional correlations with drop tests and material characterizations tests were performed.

14. SUBJECT TERMS
Crashworthiness
MC-331 Cargo Tank Motor Vehicles
White Plains, NY
Head Shielding

15. NUMBER OF PAGES
52

16. PRICE CODE

17. SECURITY CLASSIFICATION OF REPORT	18. SECURITY CLASSIFICATION OF THIS PAGE	19. SECURITY CLASSIFICATION OF ABSTRACT	20. LIMITATION OF ABSTRACT
Unclassified	Unclassified	Unclassified	UL

NSN 7540-01-280-5500 | Computer Generated | STANDARD FORM 298 (Rev 2-89)

Prescribed by ANSI Std 239-18
298-102

CONTENTS

(Continued)

(Contents continued)

LIST OF FIGURES AND TABLES

Executive Summary

Pressure Sciences Incorporated has been working under contract to the U.S. Department of Transportation (DOT) Research and Special Programs Administration to develop analytical techniques that accurately predict the response of the front head of a pressurized MC-331 cargo tank motor vehicle to collision loadings under highway crash conditions. The ultimate objective is to improve the crashworthiness of these tankers by providing practical guidance to the manufacturers to enable them to mitigate the effects of collisions with various obstacles.

Work performed by Pressure Sciences in 1996 and 1997 demonstrated the ability to use industry standard finite element analysis programs to simulate the response of pressure vessels to collisions that involve large plastic deformation of the vessel head. The contract reported herein used the tools previously developed to realistically model and analyze a propane vessel containing pressurized fluid and vapor. The results were correlated with previous tests performed circa 1970 jointly by the Railway Progress Institute (RPI) and the Association of American Railroads (AAR) and with an accident that occurred in White Plains, New York in 1994. The design of the vessel head was varied to assess the importance of essential design parameters such as head thickness and shape to the likelihood of failure under crash conditions. Then a secondary head was added in front of the front head to determine the potential for failure mitigation for dual head configurations. Finally, crushable material was added between the heads to determine its effect on failure mitigation.

This work has been discussed with individuals at the Volpe National Transportation Center to incorporate lessons learned from their work on railroad tank cars. In addition, Pressure Sciences has coordinated with a cargo tank manufacturer to ensure that the designs that were analyzed for the vessels and for the secondary head shielding were practical.

We have concluded that the incorporation of head shielding will improve the crashworthiness of the MC-331 cargo tanker, and result in fewer ruptures of the pressure boundary for the types of accidents most likely to occur. Only minor protection against normal (perpendicular) collisions with a rigid flat surface or with a rigid post oriented as a punch appears to be achievable. Protection against angled impacts into rigid surfaces or into columns of finite mass appears to be achievable by employing a secondary head. It may be further enhanced by placing energy absorbing material between the primary head and the secondary head.

Future work will be required to optimize the amount and material characteristics of the crushable material placed between the primary and secondary heads.

Correlation with accidents that have previously occurred proved to be elusive except for the White Plains accident. The types of data (speed at impact, amount of deformation, location of impact, descriptions of how the failures were initiated, etc.) that are essential to mathematically simulate the accidents were not uniformly collected. If future post accident failure teams include a structural analyst to collect this type of information, the ability to validate engineering analyses will be improved.

1 Introduction

Pressure Sciences Incorporated previously performed a feasibility study and developed analytical tools to examine the crashworthiness of front heads of DOT specification MC-331 cargo tank motor vehicles involved in highway accidents. That work was done under a contract with the U.S. DOT (Procurement Request No. 957-6177) completed June 30, 1997 and documented in Pressure Sciences report PSI-96041-005 (Reference 1). The work described in the present report follows and expands upon the work done previously. The contract statement of work (SOW) specified five requirements, which are summarized below. The contract statement of work is attached in Appendix A.

1. Perform analyses to establish correlation between analytical models and damage resulting from actual accidents. As a minimum, use as source material the accidents of 12/23/88 at Memphis, TN, 1/20/92 at Crawford, MS, and 7/24/94 at White Plains, NY. Address damage both from impact with a flat plane and with a cylindrical bridge support column of finite mass, and from puncturing forces for the typical MC-331 cargo tanks involved in the accidents.

2. In considering the puncture mode, coordinate the analytical programs employed in the feasibility study with the analytical techniques developed by the Volpe National Transportation Systems Center in their work on similar failure modes of rail tank cars. Establish appropriate failure criteria for puncture of single heads and for puncture of heads with full or partial head shields.

3. Using the results of the foregoing work, vary the head shape and thickness to determine practical designs for unprotected heads having significantly improved resistance to damage in these failure modes. Coordinate with one or more leading manufacturers of MC-331 cargo tank motor vehicles with respect to produceability and cost effects of candidate configurations.

4. Using the failure criteria established in Task 02, evaluate head shielding considering at least the following general arrangements:

   - A secondary head at various distances from the pressure-containing head;

   - A secondary head with energy-absorbing material between it and the pressure containing head.

   Produceability and cost effects of head shields are to be compared to data generated in Task 03. These findings will be coordinated with one or more leading manufacturers of MC-331 cargo tank motor vehicles.

5. Document the work in a final report.

These requirements were organized into tasks that are referenced throughout this report. The project task numbers were defined in Modification 01 to the contract (4/13/98) to better describe the sequential progress for the work. They are related to the contract statement of work as follows:

SOW Requirement	Project Task	Task Description
2	01	Work on Puncture Mode with Volpe on MC-331
1	02	Correlate Analysis with NTSB Reports
3	03	Optimize Designs Based on Work with Volpe & NTSB
4	04	Evaluate Head Shielding (Secondary) on MC-331
4	05	Add Energy Absorbing Material to MC-331
2	06	Consider Puncture Failure Modes
5	07	Final Report

Table 1: Tasks vs. Statement of Work Requirements

This report, which is project Task 07, fulfills requirement number 5 of the statement of work.

2 Review of Previous Analytical Work

Previous work (Reference 1) had compared the behavior of several pressure vessel head types (hemispherical, ellipsoidal, and torispherical heads) of various thicknesses during impact with rigid walls. Direct frontal impact and 45 degree frontal impact at speeds from 5 to 65 miles per hour (MPH) had been studied. However, as a feasibility study, the primary purpose of the 1997 work was to demonstrate the effectiveness of the proposed analytical tools and techniques for the study of, and improvement to, the crashworthiness of the MC-331 tankers. In this regard, the ANSYS and LS-DYNA engineering finite element analysis programs were shown in the 1997 study to be effective tools for assessment of impact loads and large deformation, fully plastic strains on ASME pressure vessels.

ANSYS and LS-DYNA are used in conjunction with one another because the ANSYS platform is well suited to creating the finite element models and pre-and post-processing the LS-DYNA runs. LS-DYNA is a general purpose finite element code specifically written to analyze the large deformation dynamic response of structures. Its main solution methodology utilizes explicit time integration. The advantage of the explicit method is that the finite element stiffness matrix does not need to be inverted at each time step, as is typically done for implicit solvers such as ANSYS. This saves a great deal of processing time. An explicit solution is only stable if appropriately small time steps are used in the integration. For the short dynamic transient loadings associated with the impacts studied in this report, explicit solutions are obtained much faster than implicit solutions.

One limitation of the 1997 work was that benchmarking of the prototype analysis results against test data was not included. In addition, simplifying assumptions were incorporated into the work to accommodate time and cost constraints of the contract. The most important of these assumptions were neglecting the pressure-stiffening effect of the fluid within the vessel and neglecting its mass or inertial effect.

The results nevertheless demonstrated the adequacy of the analytical approach by showing that the mathematical response of the modeled system during a collision was physically reasonable. Specifically, the deformation and force results obtained for parametric variations of the head which highway transport MC-331 tankers are subjected (high speed rollovers and striking large abutments with large mass) the failure mechanisms experienced by the railcar vessel heads and the MC-331 vessel heads are sufficiently similar to be satisfactory for benchmarking techniques.

Appendix B of the 1972 RPI-AAR report presents results of drop weight tests on $^{1}/_{12}$ scale tank car heads. These tests were chosen for our puncture mode correlation because they allowed us to investigate the effect of pressure stiffening and fluid stiffening separately. Three correlations were studied:

- unpressurized heads,
- fluid pressurized heads, and
- fluid pressurized heads with an air cushion.

After completing the initial correlation work, we met with VNTSC on July 21, 1998 to discuss the approach we were undertaking, and to review the results of their evaluations of semi-empirical analyses for rail tank car puncture velocity. The work being performed at the Volpe Center (References 3 and 4) uses a quasi-static analytical approach to determine puncture failure criteria, while this study employs a dynamic analysis approach. Both approaches are viable in their respective domains, considering the test data available for correlation. The Volpe Center has identified that the effects of fluid and pressure stiffening are important parameters that need to be considered in the crashworthiness of vessel heads and that incorporating these effects is necessary. We also obtained additional useful data from European tests documented in the Lupker paper (Reference 5), provided to us by Volpe. Further correlation studies were performed in Task 06 using the Lupker paper.

The following subsections describe in detail the process followed in validating the ANSYS/LS-DYNA modeling and analysis approach.

3.1 Correlation with RPI-AAR Unpressurized Head Drop Tests

The test setup used by the RPI-AAR in 1972 is shown Figure 1.

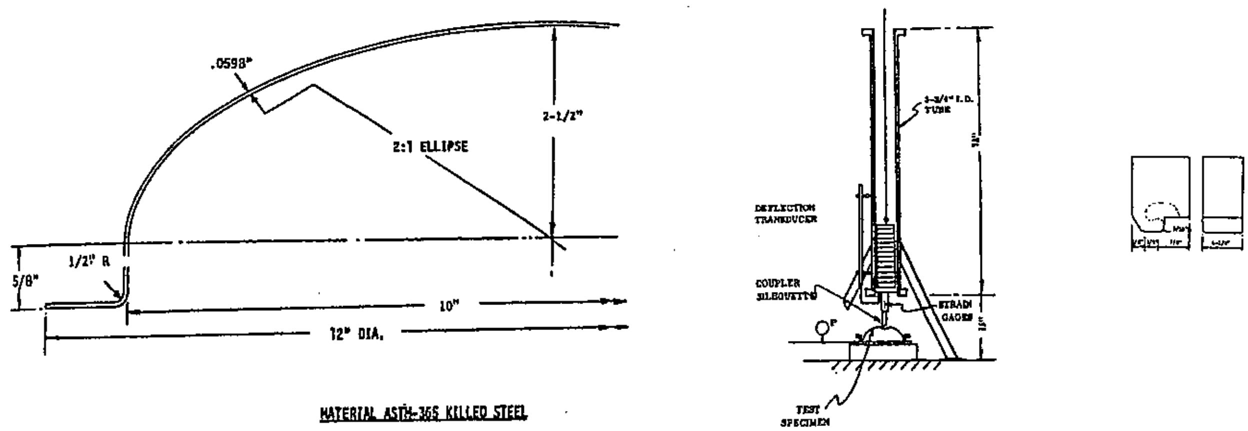

Figure 1: RPI-AAR Drop Test Configuration

thickness, shape, and speed of impact coincided with physical expectations and engineering principles. It was concluded that the ANSYS and LS-DYNA programs were viable tools for use in further detailed evaluations of specific MC-331 design and head-shielding alternatives, and they are the principal software tools used in the work reported herein.

Several issues were identified in our 1997 study that required further detailed modeling and analysis to ensure that accurate simulations of crash events were performed. The most significant issues were the stiffening effect of the propane fluid, the mass of the propane inside the tank, and the pressure of the propane. An additional objective for the current work was to accurately model a vessel colliding with a concrete column of finite mass and shear strength. Each of these items has been thoroughly examined and benchmarked against known test data and the data available from the National Transportation Safety Board (NTSB) reports.

3 Task 01: Work on Puncture Mode with Volpe Labs

Before evaluating design alternatives to improve the crashworthiness of MC-331 cargo tankers, it was necessary to validate the tools and techniques recommended from the 1997 work. The classical approach to such validation is to mathematically reproduce actual test data that have been obtained on physically similar test specimens under conditions and loadings similar to those experienced by the components under investigation. Such validation was undertaken in Tasks 01 and 06 of the current work.

There are no known, reliable, impact and puncture test data available for MC-331 specification highway cargo tanks. The bulk of the research in the area of transport vessel failure due to crash impacts has been performed for the rail transport industry, and documented by the Association of American Railroads (AAR), Railway Progress Institute (RPI) and the U.S. DOT Federal Railroad Administration (FRA). Current research focusing on methods to determine the puncture velocity of tank car shells in support of FRA programs is being carried out by the Volpe National Transportation Systems Center (VNTSC) of the U.S. DOT Research and Special Programs Administration. In order to avoid duplication of relevant work, Pressure Sciences coordinated its studies on MC-331 highway tankers with VNTSC by meeting with and exchanging information with their key personnel. In this way we have been able to incorporate lessons learned by VNTSC into the MC-331 research and extend the applicability of their results and conclusions to the unique requirements of highway transport vessels.

Pressure Sciences' Task 01 analytical work focused on demonstrating the ability to accurately predict the deformation and failure (rupture) of an ASME pressure vessel head when struck by a blunt object that is small in diameter relative to the head diameter. This configuration was selected for benchmarking because of the substantial amount of test data available from the 1972 RPI-AAR "Railroad Tank Car Safety Research and Test Project," (Reference 2). The relevant tests were $^{1}/_{12}$ scale drop tests that simulated the impact of a car coupler against a vessel head, with varying internal gas pressure and fluid content. These tests were sufficient to validate the ANSYS/LS-DYNA modeling and dynamic analysis approach, including fluid-structure interaction.

Although there are significant differences between the $^{1}/_{12}$ scale drop test conditions reported by the RPI-AAR in 1972 (simulating derailment and subsequent impact by a railcar coupler) and those to

Because of the orientation of the head, when a pressurized air cushion was included in the test, the pressurization of the internal head surface in the center impact zone was provided entirely by air. An MC-331 head would generally see pressurized fluid near the crown of the head rather than vapor. An accident is almost certain to first involve deceleration before impact. During the deceleration phase, the fluid (propane) mass can pile up against the front head, effectively creating a fluid-solid interface condition. Therefore, the water-solid condition of the drop test closely resembles the propane-solid condition that may be experienced by an MC-331 head during an accident. Nonetheless, we also calibrated the finite element model against the air cushion condition to demonstrate the viability of modeling and analyzing the gas-structure interaction under dynamic impact conditions with ANSYS/LS-DYNA.

To develop the finite element model of the test setup, it was necessary to specify the material properties of the structures and the internal fluids. Reference 2 identified the vessel head material as "ASTM-365 Killed Steel" with a tensile strength of "around 65,000 psi." No further definition of the material was provided. The ASTM A-365 specification was discontinued in 1968. Our research indicates, however, that this was a low carbon steel, with chemical composition of 0.10% C, 0.50% Mn, 0.025% max P, and 0.035% max S. Since tensile test data were not provided by the report, it was necessary to deduce the most likely strength, elongation, elastic and plastic modulus characteristics, and use these inferred properties to determine whether the finite element model was behaving properly. The best available information, which was obtained from the Metals Handbook (Reference 6) for estimated minimum properties, indicated that a yield strength of 35,000 psi and an elongation of 23% were reasonable.

No information was available for the specific behavior of the A-365 steel in the plastic region. Therefore, it was necessary to assume typical stress-strain properties, and then fine tune the properties until correlation was obtained with the results of the unpressurized tests. Because of the existing uncertainties, the most reasonable approach for this study was to specify a bilinear stress-strain curve for the analyses. For the unpressurized test configuration with no internal fluid, the material properties were fine-tuned in order to match the actual measured deflection values. The yield strength and tangent modulus were varied in the drop test analyses until the best possible correlation with a bilinear curve was obtained. The best correlation for the unpressurized heads occurred with a realistic tangent modulus of 1,050,000 psi and yield strength of 45,500 psi. Figure 2 shows the correlation between the 1972 data from the unpressurized tests and the ANSYS/LS-DYNA analyses.

The drop test correlation model shown in Figure 2 used ANSYS/LS-DYNA explicit shell elements (type 163). An option with the element formulation was invoked so that warpage (i.e., nodes of an element not in a flat plane) of the finite elements was correctly accounted for in the solution. The impacting coupler was modeled using explicit solid elements (type 164) and explicit mass elements (type 166). A bilinear isotropic hardening plasticity material model was used. The ANSYS/LS-DYNA finite element model is shown in Figure 3.

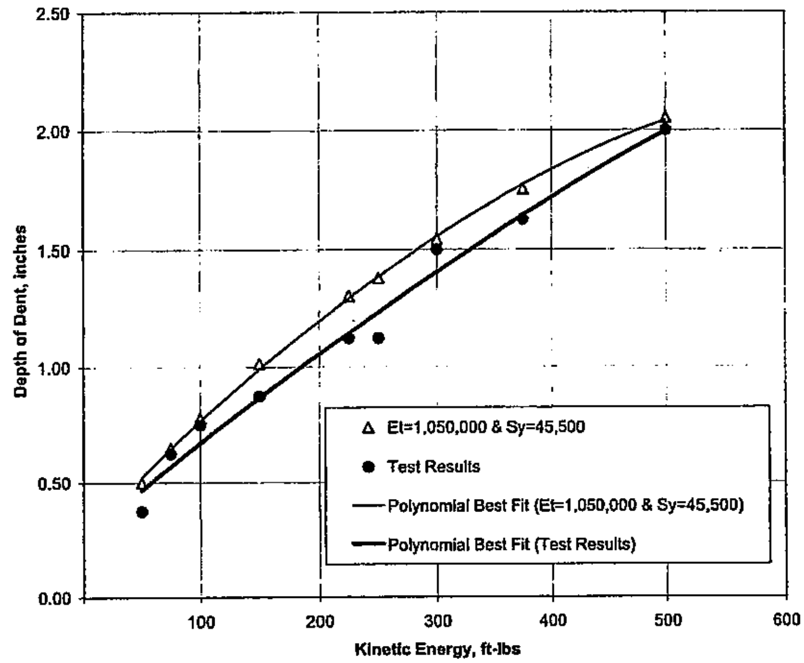

Figure 2: Correlation with Drop Tests using Unpressurized Heads

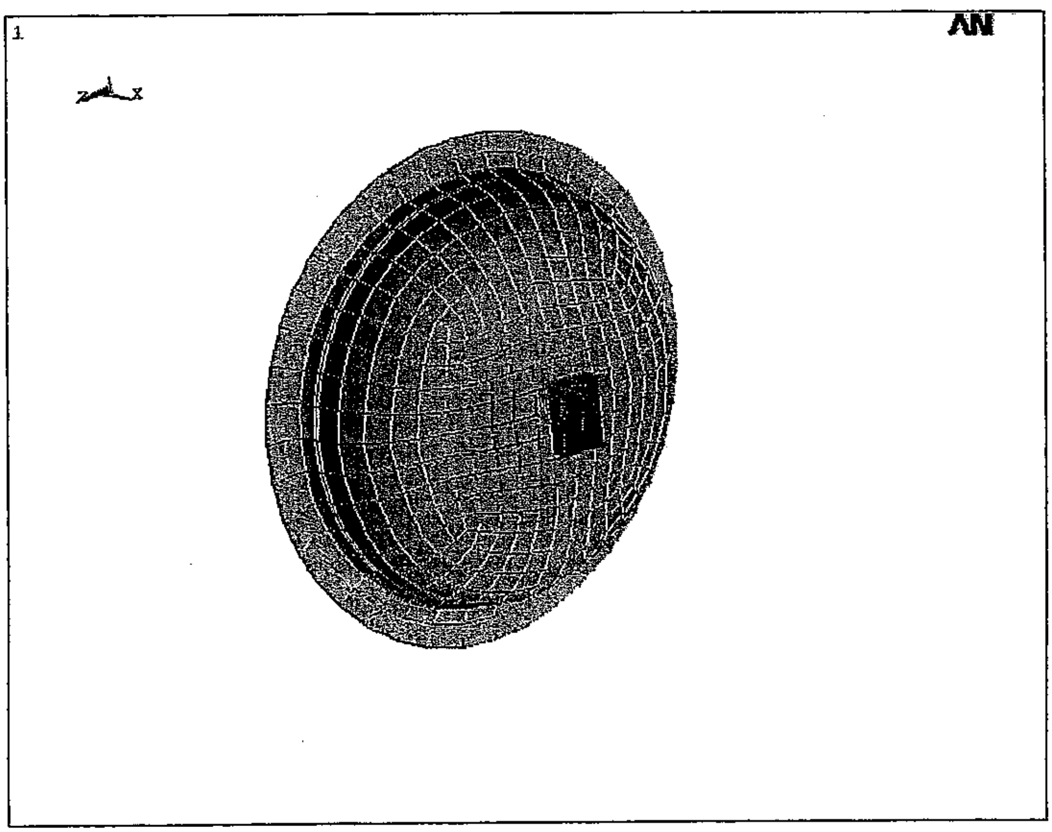

Figure 3: Finite Element Model Used for Unpressurized Drop Test Correlations

3.2 *Correlation with Pressurized Drop Tests*

The modeling of the gas pressure, without consideration of the stiffening effects of the water, was the next step. This would have been equivalent to a 100% air cushion in the 1972 test configuration, but no such configuration was tested. It is only known that a pressurized air cushion over the water existed, but the extent of the air cushion (percent air vs. percent water) was not specified in the report. Regardless, modeling the gas pressure was a necessary first step to including both liquid and vapor phase components.

We modeled the pressure load using both the implicit-to-explicit sequential solution technique and the dynamic relaxation technique. In the implicit-to-explicit solution technique, the model is solved using ANSYS implicit elements and then a restart analysis is performed in LS-DYNA using explicit elements and the implicit solution. In the dynamic relaxation technique, the pressure is applied to the explicit elements and LS-DYNA increases the damping until the kinetic energy becomes approximately zero.

As seen in Figure 4, the modeling of the gas pressure alone, without modeling the water, (the upper curve) overestimated the calculated deflection (dent depth) as compared to the actual test data (the lower curve). This indicated that the stiffening effect of the liquid was significant in reducing the calculated deflections, and inclusion of this effect is necessary.

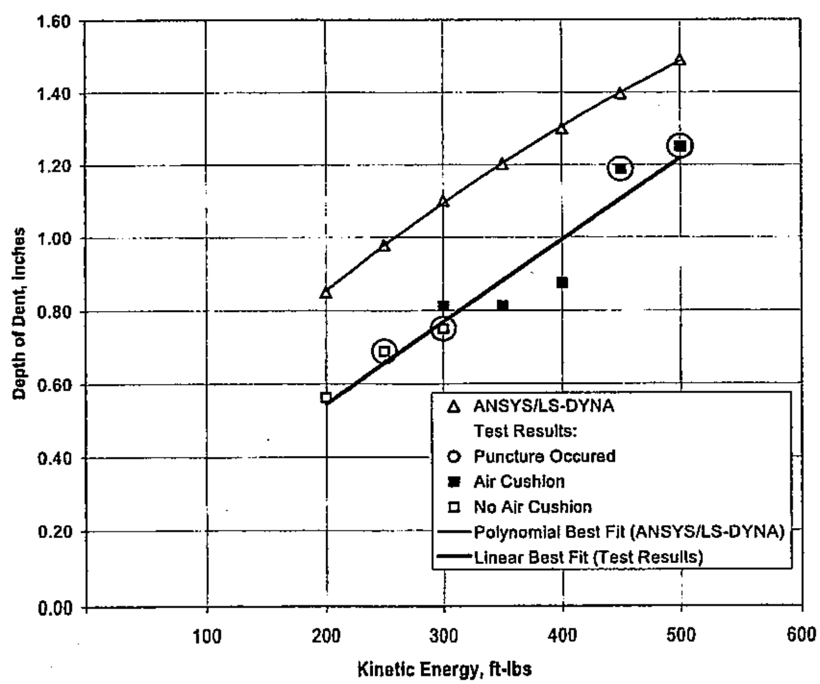

Figure 4: Correlation without Fluid Elements with Drop Tests using Pressurized Heads

In order to improve the correlations with the pressurized head tests, the water had to be explicitly included in the finite element model.

3.3 LS-DYNA Fluid Model

In order to model the liquid water, explicit solid elements (type 164) were used for the water. The material model used for the water was the elastic material model with the fluid option.

The air/vapor cushion was modeled using explicit solid elements (type 164) and the null material model with a linear polynomial equation of state.

In the LS-DYNA Theoretical Manual (Section 17.1, Reference 7), it is shown that one form of the equation of state is the linear polynomial shown below, which is linear in terms of internal energy per initial volume. This is the most applicable form for the analyses being considered.

$$P = C_0 + C_1\mu + C_2\mu^2 + C_3\mu^3 + (C_4 + C_5\mu + C_6\mu^2)(E),$$

where:

$\mu = (\rho/\rho_0) - 1,$

ρ/ρ_0 is the ratio of current density to initial density,

$\mu = (1/V) - 1,$

V is the relative volume, and

E = Internal energy per initial volume, pressure units.

For this so-called Gamma Law equation of state, Section 27.2 of the LS-DYNA Theoretical Manual states that the derivation is obtained from adiabatic expansion of an ideal gas.

$$p=(k-1)\rho e$$

where:

p = pressure

k = specific heat ratio ~ 1.4 for air as an ideal gas

e = specific internal energy

For the Gamma law equation of state:

$$C_0 = C_1 = C_2 = C_3 = C_6 = 0,$$
$$C_4 = C_5 = (k-1) \sim 0.4 \text{ for air as an ideal gas}$$

Then the pressure is given by

$$P = (k-1)(\rho/\rho_0)(E) = (k-1)(1/V)(E)$$

We initially used the Gamma Law equation of state, but were not satisfied with the pressures produced. (It was later determined that an error exists in the LS-DYNA solver (version 940.2) when 8-point integration null elements are used). Therefore, we subsequently used a simplified version of the linear polynomial equation of state to simulate Boyle's Law ($P_1V_1 = P_2V_2$), which requires that the system be isothermal. For the short duration of the impact, there is no practical difference between the isothermal assumption and the adiabatic assumption.

Since

$C_2 = C_3 = C_4 = C_5 = C_6 = 0$, then
$P = C_0 + C_1\mu + C_2\mu^2 + C_3\mu^3 + (C_4 + C_5\mu + C_6\mu^2)(E)$ becomes
$P = C_0 + C_1\mu$
$P = C_0 + C_1[(1/V) - 1] = C_1/V + (C_0 - C_1)$

Let $(C_0 - C_1) = -14.7$, the correction from absolute pressure to gage pressure.

$P = C_1/V$ is Boyle's law

Figure 5 shows the test model that was used to validate the simplified equation of state developed above. The model consists of fluid elements surrounded by shell elements, with the first row of fluid elements replaced with the simplified equation of state elements. C_0 was set to 100 psig and C_1 was set to 114.7 psia. The resulting stresses in the shell elements confirmed that an initial internal pressure of 100 psig was developed.

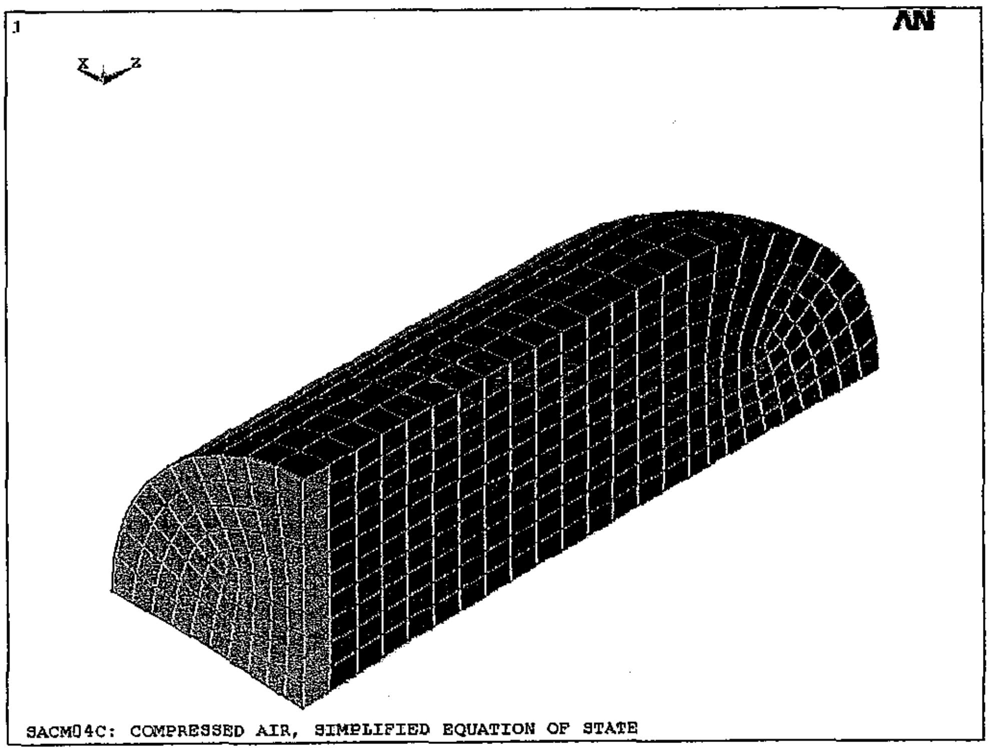

Figure 5: Model Used to Validate Simplified Equation of State

A second test model using two arbitrary zones of pressure was used to further validate the simplified equation of state model. The first zone was at 85.3 psig (100 psia) and the second zone was at 35.3 psig (50 psia). The combined pressure expected was 60.3 psig and the shell stress results from the analytical model corresponded to an internal pressure of 60.0 psig, again verifying the validity of the simplified equations developed.

The simplified equation of state was then used to model a 10 percent air cushion into the drop test model. The remaining 90 percent of the interior of the model consisted of elastic material with the fluid option as shown in Figure 6. The correlation of the finite element model that includes fluid elements with the actual drop tests is shown in Figure 7.

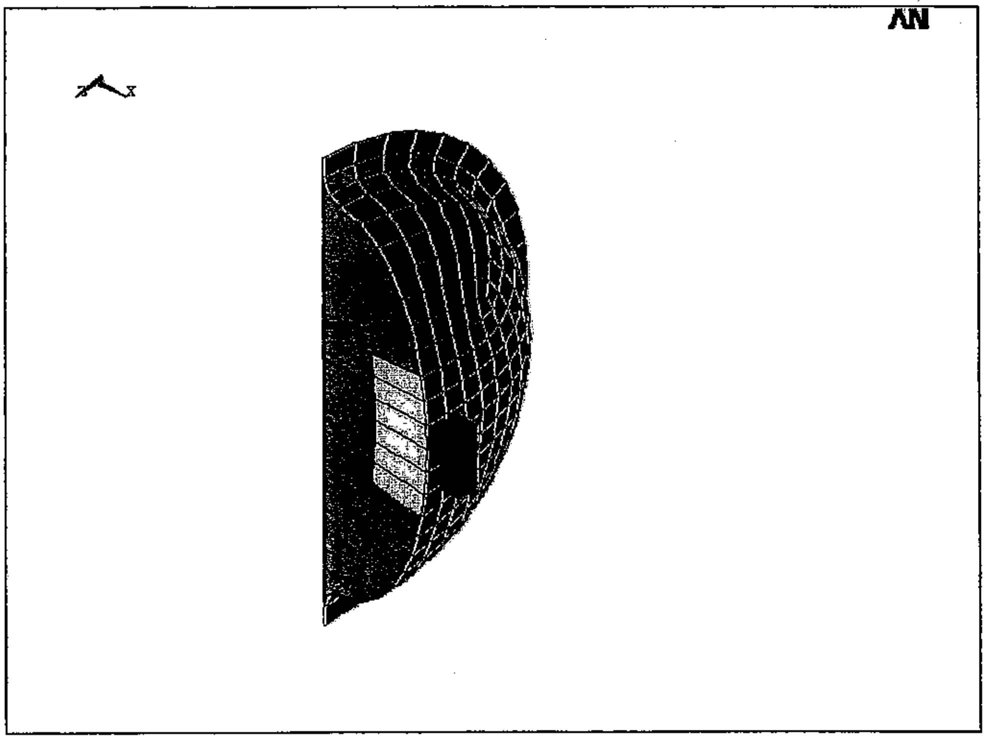

Figure 6: Finite Element Drop Test Model with Fluid Elements

Figure 7 includes the unpressurized results from Figure 2 to illustrate the stiffening effect caused by pressurization. The analytical results with and without the 10 percent air cushion bound the results from the tests conducted with an air cushion. In the analytical model, the impacting coupler rebounded after impact with the shell. The dent depth values presented in Figure 7 are the values calculated after elastic rebound, except for those labeled, "Max D". The "Max D" values are the maximum deflections that occur during impact, including elastic deflections. It is interesting to note that the "Max D" values correlate well with the measured deflections from tests in which puncture occurred.

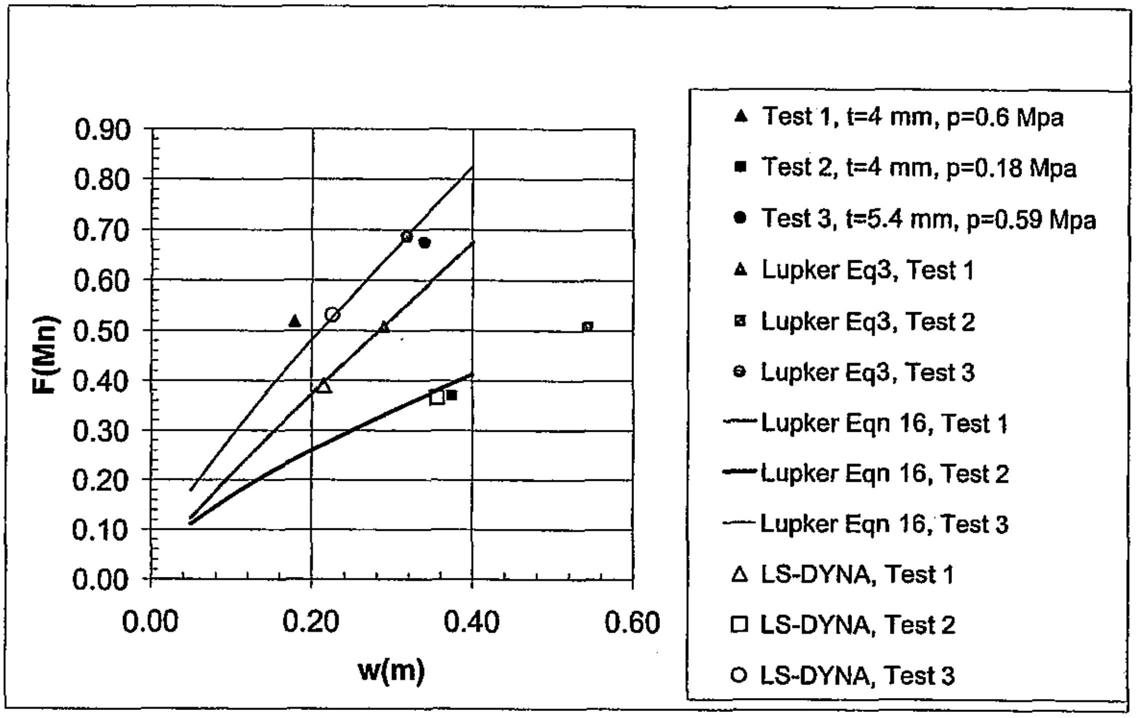

Figure 8: Correlations Between Lupker Data and ANSYS/LS-DYNA Models

This correlation shows very good agreement between the force-deflection relationship developed by Lupker (Equation 16) and the LS-DYNA force-deflection results. However, it should be noted that Lupker's Equation 16 is undefined when the pressure is greater than one-sixth of the ultimate capacity under internal pressure; and therefore it cannot be used to evaluate heads constructed with a safety margin of less than six against pressure. Furthermore, Lupker's Equation 3 for the force needed to cause puncture is not a function of pressure, as can be see by comparing the Equation 3 values at pressures of 0.6 MPa (Test 1) and 0.18 MPa (Test 2) in Figure 8.

Lupker's force to cause puncture given in his Equation 3 is approximately equal to the product of the perimeter of the penetrating object, the ultimate transverse shear strength of the material, the thickness and a coefficient determined from the experimental results. Because his Equation 3 is an empirical formula based upon data from tests 1 and 3, there is a close correlation between Lupker's Equation 3 and the measured puncture forces. However, for test 2, Lupker's Equation 3 over-predicted the puncture force, while the ANSYS/LS-DYNA results are within one percent of the measured value.

The VNTSC evaluation of semi-empirical analyses (Reference 4), such as Lupker's, determined that the use of transverse shear as a failure criterion is consistent with the assumed material model. VNTSC further notes that using the transverse shear as a failure criterion with an elastic-plastic material model is inappropriate. VNTSC results suggest that plastic strain is an appropriate failure criterion when performing elastic-plastic analyses. Since elastic-plastic material models were used in our ANSYS/LS-DYNA analyses, we developed failure criteria based upon the effective plastic strain at failure as discussed in Section 6.2.

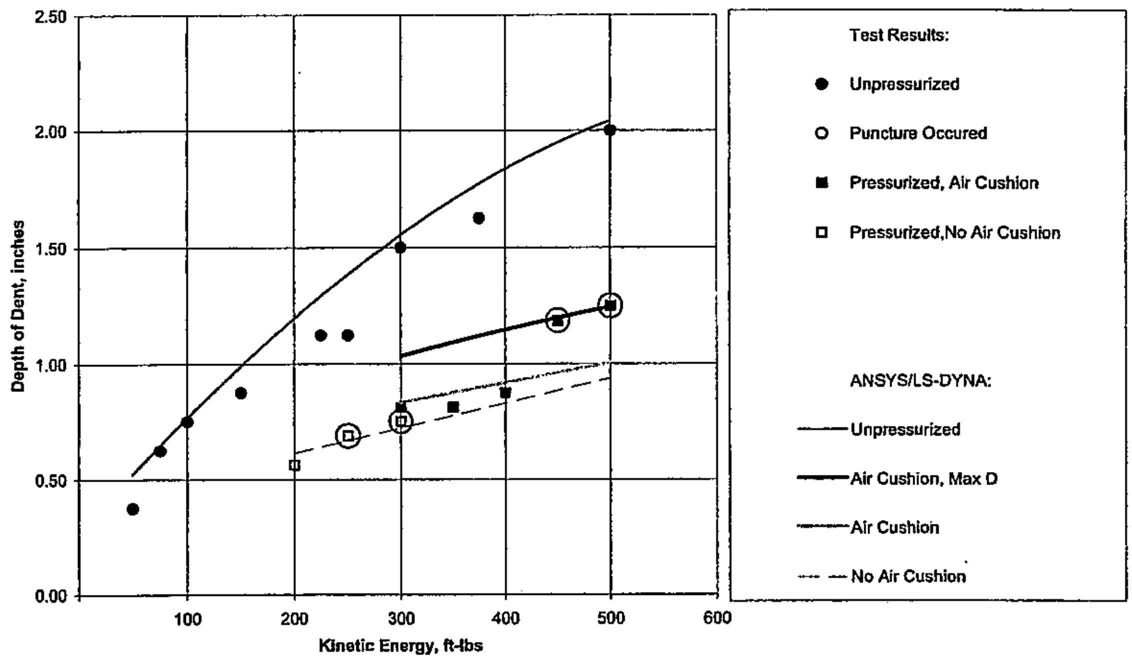

Figure 7: Correlation with Fluid Elements with Drop Tests using Pressurized Heads

Because of their low density, the elements used to model the air cushion were extremely prone to hourglassing. Hourglassing modes are the zero energy modes, which arise when using one-point Full integration elements were therefore used for the air cushion to eliminate the hourglassing effects, even though this required substantially longer run times. Alternatively, the one-point integration elements could have been used with an exact integration B matrix. Closed form expressions for the terms in the B matrix are given in Reference 9. The exact integration B matrix is achieved in LS-DYNA by using type 3 hourglass control and setting the hourglass parameter to a small number (e.g.10^{-6}).

4 Task 06: Consider Puncture Mode Failures

The activities required to complete milestone 06 are closely related to those of milestone 01. Therefore, for project continuity, work on Task 06 followed Task 01, and is presented as such in this report.

4.1 Correlation with Lupker Data

As stated earlier, Pressure Sciences obtained the Lupker paper (Reference 5) from VNTSC. This paper provided another source for test data on pressurized transport tank heads. The correlation of ANSYS/LS-DYNA dynamic analysis results with the empirical equations developed by Lupker is shown in Figure 8.

4.2 Puncture Mode Failure Criteria for MC-331 Heads

As the result of analytical work performed in Tasks 01 and 06, it was concluded that an appropriate failure criterion for puncture could be based upon the effective plastic strain that occurs at failure of a uniaxial test specimen.

We developed the following procedure under Task 06 to evaluate the ability of the heads to withstand puncture failure.

1. Select an appropriate penetrating shape. Although somewhat arbitrary, a 6 inch circular rigid bar seems appropriate for the evaluations required for Tasks 04 and 05.

2. Model the MC-331 tank shell and head using a bilinear stress-strain material curve with strain hardening characteristics.

3. Model the fluid using finite elements that have low shear stress and are highly incompressible. Pressure Sciences has shown that LS-DYNA material model 1 with the FLUID option is found to be well suited for this.

4. Refine the finite element mesh near the circumference of the anticipated penetrating contact to enable accurate strain evaluations.

5. Apply the appropriate velocity to the MC-331 tank and contents.

6. Use the eroding element capability of ANSYS/LS-DYNA to "fail" elements whose effective plastic strain exceeds the effective plastic strain criterion developed in Section 6.2.

In order to evaluate the effectiveness of designs to mitigate puncture failure we used the procedures developed under Task 06 to evaluate the secondary head shielding (Task 04) and the effectiveness of the addition of energy absorbing material (Task 05).

5 Task 02: Correlate Analyses with NTSB Reports

Having obtained reasonable correlation with the drop tests, we now began the task of correlating the calculated effects of the impact of the propane tanker truck with the effects observed in the NTSB reports.

Information on the following accidents was reviewed:

- 12/23/88 Memphis, TN
- 01/20/92 Crawford, MS
- 07/27/94 White Plains, NY

The report of the Crawford, MS accident did not provide enough data to produce an analytical correlation. However, it was the accident that led us to consider angled impact with a rigid wall.

The White Plains, NY accident report (Reference 8) was the only one to provide sufficient information to enable a valid analytical correlation. At impact, the propane trailer was traveling at 37 MPH and struck a circular concrete column with a static shear capacity of 210,000 lbs. The combined weight of the vehicle and cargo was 80,160 pounds, and the weight of the portion of the column that was sheared off was estimated to be 13,230 pounds. The front head of the tank buckled and fractured, releasing the propane, which vaporized into gas. The resulting vapor cloud expanded until it found a source of ignition and ignited. The tank was propelled some 300 feet.

ANSYS/LSDYNA was used to develop a 3D finite element model of the complete propane tank, the propane liquid, and the propane gas. The trailer and tractor were modeled as lumped masses attached to the bottom of the propane tank. The concrete column was modeled as a rigid body with a breakaway force of 210,000 lbs. Figure 9 shows the total strain in the front head for impact with a concrete column that does not break away. Figure 10 shows the total strain in the front head for impact with a concrete column with a shear capacity of 210,000 lbs.

The mesh size used for the models shown below was the same mesh size that was used in Reference 1. Under Task 03, an improved model with a smaller mesh size was developed and evaluated to determine whether the predicted plastic strains can be better correlated to the failure strains for SA 517 material by using a finer mesh.

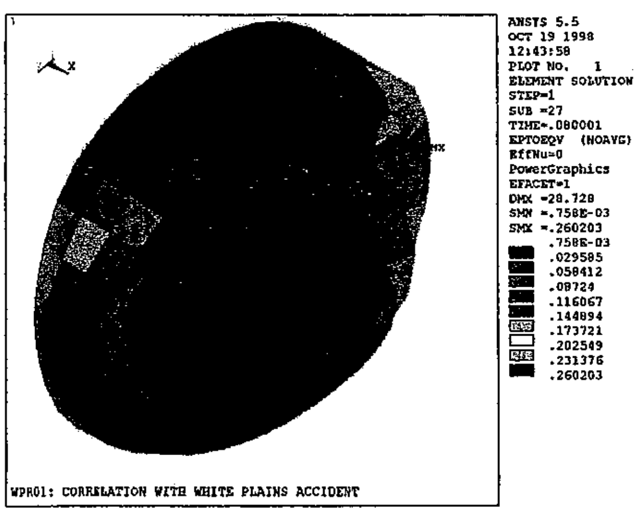

Figure 9: Impact with Concrete Column/No Break Away

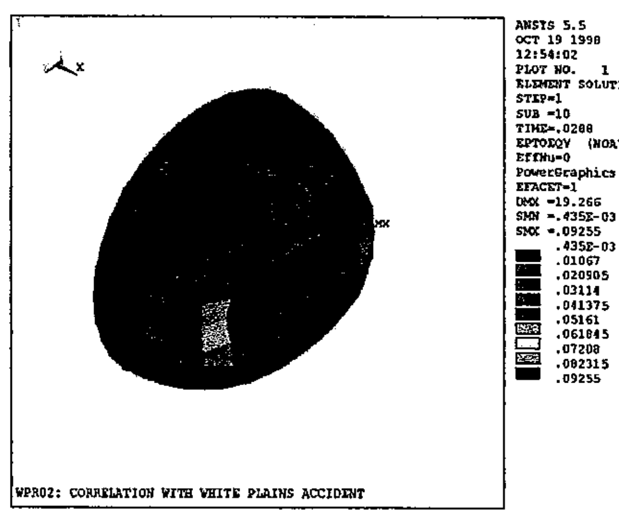

Figure 10: Impact with Concrete Column/Shear Capacity of 210,000 lbs.

Figure 11 shows the complete ANSYS/LS-DYNA model that includes the propane tank, the propane liquid and the propane gas. Because we were unable to obtain a value for the bulk modulus for propane, we used the bulk modulus of water as a reasonable estimate for the propane. The trailer and tractor were modeled as lumped masses attached to the bottom of the propane tank. The concrete column was initially modeled as a rigid body, with a breakaway force of 210,000 pounds represented by a fictitious spot weld acting as a mechanical fuse. The column was modeled as a rigid body constrained in all directions except the direction of impact. Since a spot weld cannot be directly connected to a rigid body, fictitious stiff beam elements with low density were attached to the column and a spot weld with the break away shear force was added between the beam elements.

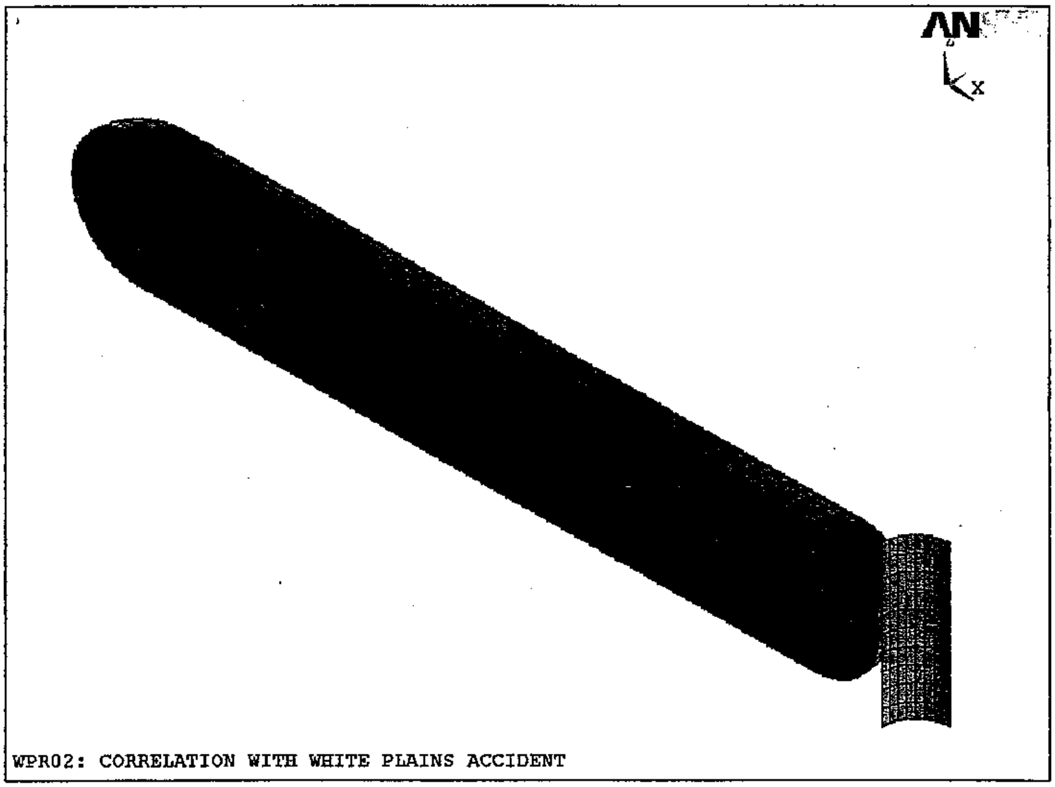

Figure 11: Propane Tank, Liquid, and Vapor Model

The initial evaluations produced buckling of the front head that was remarkably similar to the buckling that actually occurred, as shown in photographs in the NTSB report. However, the amount of hourglassing energy associated with the liquid propane elements was greater than 10 percent of the internal energy. Hourglass control Type 5, Flanagan-Belytschko stiffness form with exact volume integration for solid elements, was used to reduce the hourglassing energy of the liquid propane elements. This particular type of hourglass control, however, had the adverse effect of eliminating the buckling, or folding of the front head. In order to eliminate the hourglassing energy and still obtain good correlations with the observed behavior, full integration elements were used for the liquid propane. It was subsequently determined that one-point integration elements with an exact integration B-matrix (as described at the end of Section 3.3) gave similar results to the full integration elements with substantially reduced run times.

When the breakaway force of the concrete column was set to 210,000 pounds, the amount of permanent deformation of the tanker was 6.5 inches, which was smaller than the observed deformation of 21 inches. If the concrete column was modeled with an infinite breakaway force, the amount of permanent deformation of the tank head was 38 inches. However, it was observed that the maximum force generated at the spot weld for this case was slightly greater than 3,000,000 pounds. When a breakaway force of 3,000,000 pounds was used, the amount of permanent deformation was 19.5 inches.

Note that it is common for a stationary object such as the concrete column to seem much stronger under dynamic loading than it does under static loading. Impact energy is transmitted in all directions at the speed of sound. The larger the object struck, the more time it takes to reach distant locations, the more diffuse the energy is, and the more excess energy that is required to produce failure. It is not surprising that the concrete column exhibits a high ratio of dynamic to static failure load.

We wanted to run several models with various head shapes and various thicknesses to determine if the crashworthiness of the propane tank head could be improved. In order to reduce the runtimes associated with the finer mesh size required to calculate accurate strains, a reduced model of the front head was developed that incorporated ¼ symmetry. Since a cylindrical steel vessel of length greater than 4.9 $(rt)^{0.5}$ acts as if it were infinitely long, the shell length included was greatly reduced. The mass of the remainder of the vessel and propane was modeled by increasing the density of the last row of elements. Furthermore, in the reduced model the elements used to model the propane vapor were replaced with a surface pressure loading and balancing nodal forces at the last row of elements.

Figure 12 shows the reduced model of the head that buckled and produced a permanent deformation in the head of 19.5 inches. The 23% maximum strain observed in this analysis, when compared to the specified 16% minimum elongation for the head material, is indicative of likely failure. This model indicates good correlation with the actual permanent deformation of 21 inches of the buckled head and has strain values that are consistent with the failure observed.

In summary we were able to use ANSYS/LS-DYNA to obtain good correlations with drop tests when we modeled the liquid propane using the elastic material model with the fluid option, and modeled the propane vapor with a null material with the linear polynomial equation of state. We also obtained reasonable correlations with the White Plains, NY accident involving a propane trailer when we accounted for the liquid propane as described above and modeled the concrete column using rigid elements with a finite breakaway force.

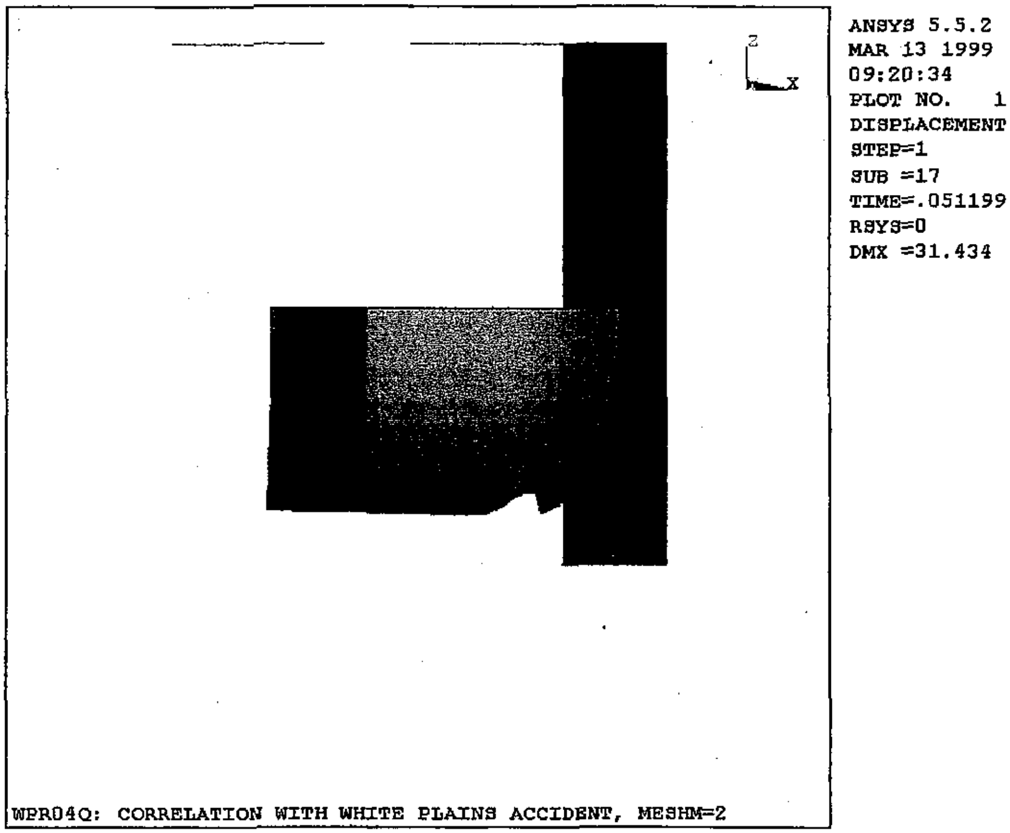

Figure 12: Buckling in Model of Propane Tank Head

6 Task 03: Optimize Designs Based on Correlations with Volpe Work and NTSB Reports

The goal of this task was to optimize the bare (unprotected) head designs by varying the head shape and thickness for practical designs to determine if significantly improved resistance to failure can be achieved. The base design was considered to be a 0.250 inch thick hemispherical head, which is typical for MC-331 cargo tanks. For an inside radius of 41.75 inches, a design pressure of 250 psig and an allowable stress value of 28,800 psi (allowable stress value for SA517 material not considering the recently increased stress levels in ASME Section VIII, Division 1), the required corresponding cylinder thickness is 0.364 inch. For the second design evaluation, it seemed reasonable to choose a hemispherical head with a thickness matching the required cylinder thickness. However to allow for comparisons with our previous report, a slightly greater thickness of 0.378 inch was used for the thickness of the second hemispherical head. The third design alternative chosen was an ellipsoidal head with a minimum required thickness of 0.363 inch. The fourth bare head design alternative was a torispherical head. Changes recently adopted by the ASME Boiler and Pressure Vessel code allowed the torispherical head thickness to be 0.757 inch rather than the thickness of 0.946 inch that would have been previously required; and this smaller thickness was used.

The following scenarios were considered.

1. The heads impacted an immovable flat plane head-on.
2. The heads impacted an immovable flat plane at a 45-degree angle.
3. The heads impacted a 6 inch diameter immovable circular post in line with the centerline of the vessel.
4. Finally, the heads impacted a 42 inch diameter cylindrical column of finite strength and mass after the cargo tank had turned on its side, with the centerlines of the tank and the column perpendicular to one-another, as occurred in the White Plains accident.

In order to simplify our evaluations in the feasibility study conducted under our previous contract with the U.S. Department of Transportation, we had neglected the effects of the propane inside the tank. In this task, in order to improve the accuracy of the results, we have included the normal operating pressure of the propane gas and the mass of the propane and the momentum it adds to the impacting trailer.

The mesh size of the model created under Task 02, "Correlation with NTSB Reports," was reduced to improve the correlation between the strains calculated and the failure strains for SA517 material. In order to solve the models with the smaller mesh size, quarter symmetry models and simplified models that use lumped masses for the rear head and the majority of the cylindrical shell were also developed. Section 5 indicates that these smaller models accurately predict the response of the full sized model.

6.1 Development of Evaluation Criteria

Our initial analyses for this task were conducted at only 35 and 55 MPH. These analyses indicated significantly higher strains for a given speed than previously reported and indicated the difficulty in providing protection from the failure modes considered with bare heads.

These initial analyses also indicated the need to consider using accumulated plastic strain rather than total strain as the criteria for failure. The equivalent total strain in an analysis with plasticity needs to account for the increase in Poisson's ratio that occurs after yielding. The accumulated plastic strain method internally accounts for the increased Poisson's ratio whenever plasticity occurs. Furthermore, ANSYS/LS-DYNA includes the ability for elements to erode or "fail" if their accumulated plastic strain exceeds a given value. This allows for progressive failure, which was useful for the head shielding evaluations where the secondary head was sacrificial.

The effective plastic strain failure value was determined from the minimum required properties for SA-517 material shown in Table 2.

Yield Strength	Ultimate Strength	Elongation in 2 inches
100,000 psi	115,000 psi	16 percent

Table 2: Minimum Specified Properties for SA-517 Material

The 16 percent elongation in 2 inches corresponds to the amount of plastic engineering strain. Using an assumed elastic Young's modulus of 30,000,000 psi, the elastic engineering strain at failure would be 115,000/30,000,000 or 0.0038 in/in. Therefore, the total amount of engineering strain in a uniaxial test is 0.1638 in/in (16% plus 0.0038). Since ANSYS/LS-DYNA uses true stress and true strain, the engineering stress and strain values were converted to true values. The true strain and true stress values at yield and ultimate strength conditions are given in Table 3. Since a bilinear stress-strain curve is used, necking cannot be accounted for in the true stress and strain calculations. The tangent modulus (E_{tan}) for the bilinear stress vs. strain curve was calculated from the true stress and strain values given in Table 3 to be 225,805 psi.

Engineering Stress (psi)	True Stress (psi)[1]	Total Engineering Strain (in/in)	Total True Strain (in/in)[2]	Elastic True Strain (in/in)[3]	Plastic True Strain (in/in)
100,000	100,333	0.0033	0.0033	0.0033	0.0000
115,000	133,841	0.1638	0.1517	0.0038	0.1473

Table 3: True Stress and Strain Values for SA 517 Material

The validity of the bilinear stress versus strain curve was confirmed by creating an ANSYS/LS-DYNA model of a 6 inch by 1 inch by 0.25 inch thick plate and applying a displacement of 0.983 inches, which corresponds to a total engineering strain of 0.1638 in/in. The total effective plastic strain calculated by ANSYS/LS-DYNA was between 0.1469 and 0.1476 in/in. The reaction force generated at the fixed end was 28,744 pounds, which corresponds to an engineering stress of 114,976 psi.

Having confirmed the values that are shown in Table 3, the remainder of the models were created using an effective plastic strain failure criterion value of 0.1473 in/in and a tangent modulus of 225,805 psi.

Another change that was made under this task was a switch from isotropic hardening material models to kinematic hardening models. This change was made because kinematic hardening predicts a Bauschinger effect (i.e., the range of elastic stress remains approximately twice the yield stress under cyclic loading) as observed in real materials, while isotropic hardening does not include the Bauschinger effect. This is important in head failure evaluation because portions of the head fold and unfold as the collision proceeds.

By incorporating a failure strain criteria and eroding elements, the maximum effective plastic strain for any given run was now limited to the effective plastic strain failure value. Therefore comparing the amount of effective plastic strain calculated for various designs at a given speed was not very useful if failure occured. A more useful means of comparing the various designs was to determine

[1] $\sigma_t=\sigma_e(1+\varepsilon_e)$, subscripts indicate true or engineering values

[2] $\ln(1+\varepsilon_e)$

[3] Elastic true strain=σ_t/E

the lowest speed at which the surface strains equaled 0.1473 in/in, the failure strain. The various design alternatives were analyzed in 5-MPH increments. This was done because determining precise failure speeds is an iterative process that consumes too much computer run-time and is not practical. In ANSYS/LS-DYNA, an element is not eliminated until the top, middle and bottom surface strains equal the failure value. For purposes of comparing the various design alternatives, the lowest failure speed was taken as the speed at which either the top or the bottom surface strains equaled the failure value.

6.2 Conclusions Regarding the Bare Head Designs

Appendix B gives a summary of all the design alternatives, including head shielding and the addition of energy absorbing material. For all the bare head designs and all the impact scenarios, failure would be expected at or below 30 MPH.

6.2.1 Impact into a Rigid Wall

The base design (0.250 inch thick hemispherical head) failed at approximately 25 MPH when striking a rigid wall as shown in Figure 13. The undeformed mesh size is shown in Figure 14. The mesh size shown in Figure 14 is smaller than the mesh size shown in Figure 9. A further mesh refinement study, using half this mesh size, as shown in Figure 15, indicates that failure might be expected at speeds as low as 15 MPH. The computational time required for the mesh density of Figure 14 was 987 seconds, while the computational time required for the mesh in Figure 15 was 37,704 seconds. In order to perform a comparative analysis for the various design alternatives, over 200 analyses were required. Therefore the computationally efficient mesh density shown in Figure 14 was used for most of the analyses. For the 0.363 inch thick ellipsoidal head, the failure speed of 25 MPH was the same for both mesh densities.

The results for the differing head designs indicate little or no difference between them for the case of frontal collision into a rigid wall. Note that this and the penetration case assume perfectly head on collisions with immovable rigid objects. Actual accidents in all likelihood will be much less severe.

Simply put, the analyses in this report are valid for comparing one geometry with another; the finer mesh density may be needed to obtain more accurate failure speeds for a given geometry.

An interesting result of the analysis was that the thicker hemispherical head indicates a lower failure speed than the thinner head, when both strike a rigid wall. This same trend appeared during the mesh refinement study discussed previously. We believe that this trend is explained by considering the bending of a plate through a given angle. For a given bend angle, a thicker plate will be subjected to greater unit strain on the outside and inside surfaces than a thinner plate. When the hemispherical head strikes the rigid wall, the impacting force tends to flatten the head out over the area of contact, resulting in a sharp bend radius at the edges of the flattened region and higher strains for thicker plates. For the ellipsoidal and torispherical heads, this effect is not as severe, because their crown radii are larger, and the bend angles are not as great.

The failure of the base design at 25 MPH, was a failure of only one surface of the plate elements, or a partial failure. Full failure of the 0.250 inch thick hemispherical head was not indicated until velocity was greater than 35 MPH.

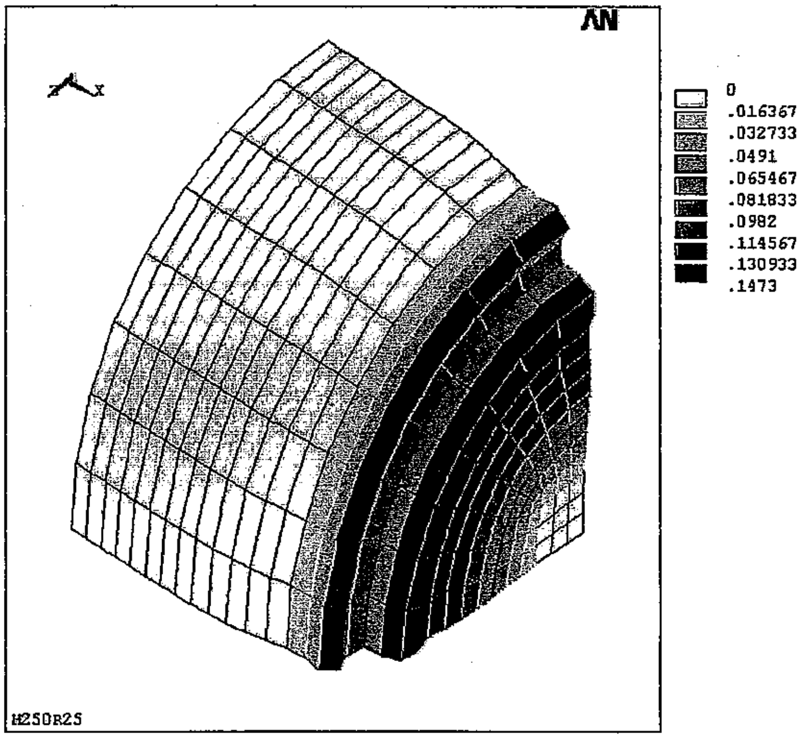

Figure 13: Effective Plastic Strain of 0.25 Inch Thick Hemispherical Head Impacting Rigid Wall at 25 MPH

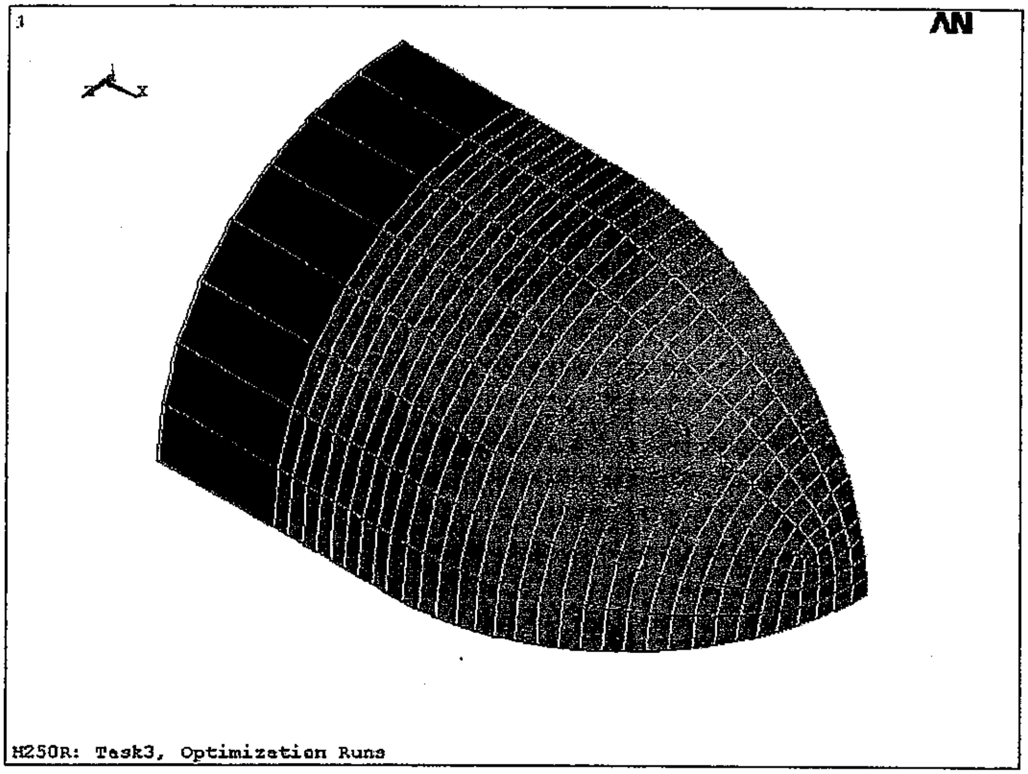

Figure 14: Mesh Density Used for the Comparative Study

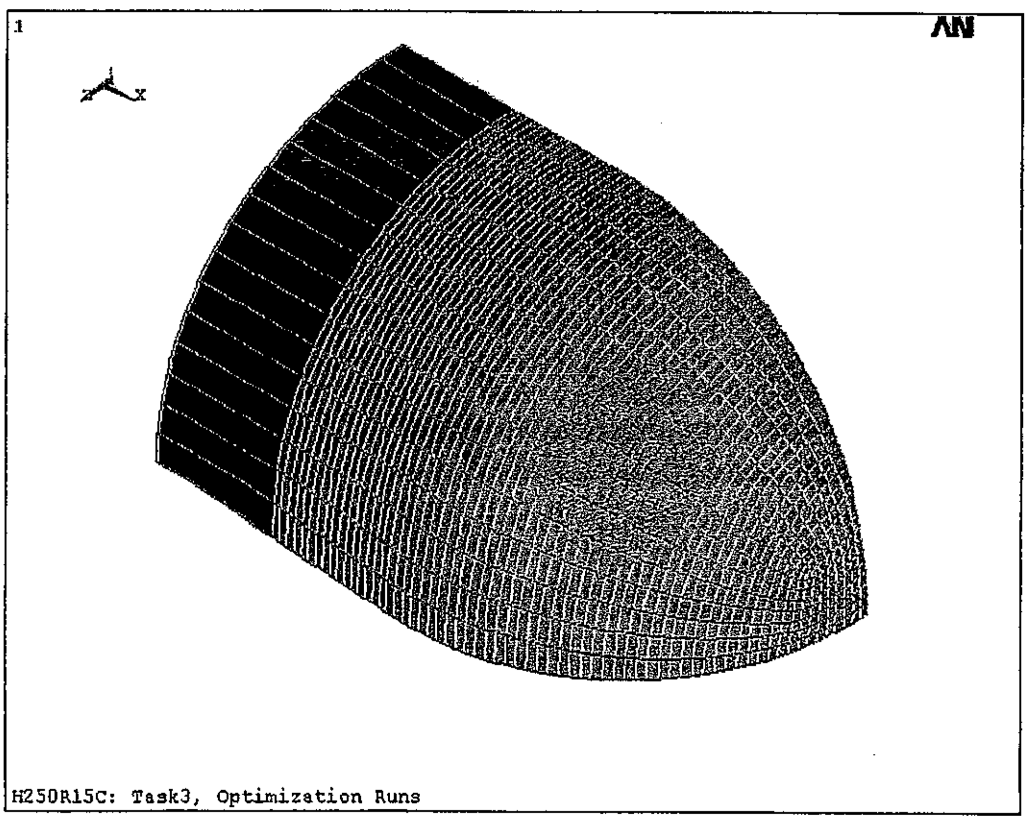

Figure 15: Twice the Mesh Density Used for the Comparative Study

6.2.2 Angled Impact into a Rigid Wall

In our opinion, the scenario of a tank truck striking a rigid wall at an angle is a more realistic scenario to evaluate the design variations, since it is more representative of the types of accidents that are likely to occur.

The speed at which failure occurred, when considering angled impact into a rigid wall, was 25 MPH for the hemispherical (see Figure 16) and ellipsoidal heads. Failure of the torispherical head occurred at 15 MPH. For the ellipsoidal head, failure strains were observed in the shell and not in the head at 25 MPH. For the torispherical head, the highest strains were observed in the sharply curved knuckle radius region.

6.2.3 Penetration Impact

For the bare head designs, failure occurred at or below 5 MPH when they collided in a punching mode with an immovable 6 inch diameter post, as shown in Figure 17. Unlike the other impact scenarios considered, the penetration analysis indicated that there was very little discernable difference between the speed at which failure of one surface was initiated and the speed at which complete failure occurred. For the torispherical head, partial failure occurred below 5 MPH and full failure occurred below 10 MPH. For the other head designs partial and full failure occurred below 5 MPH.

6.2.4 Impact into a Column of Finite Strength and Mass

An accident scenario involving a tank truck head striking a concrete column was developed based upon the data from the White Plains accident. The shear strength of the column was set as discussed in Section 5; and failure of the column did not occur until it was struck at approximately 30 MPH. The actual speed at which the column failed varied for the different head designs evaluated because of the varying amounts of energy absorbed by the tank truck heads. For the bare head designs, the heads began to fail before the column broke away. The 0.25 inch and 0.378 inch thick hemispherical heads failed below 15 MPH (see Figure 18), with the ellipsoidal head failing below 20 MPH, and the torispherical head failing below 25 MPH. The corresponding columns failed below 30 MPH, below 20 MPH, above 30 MPH and below 25 MPH, respectively.

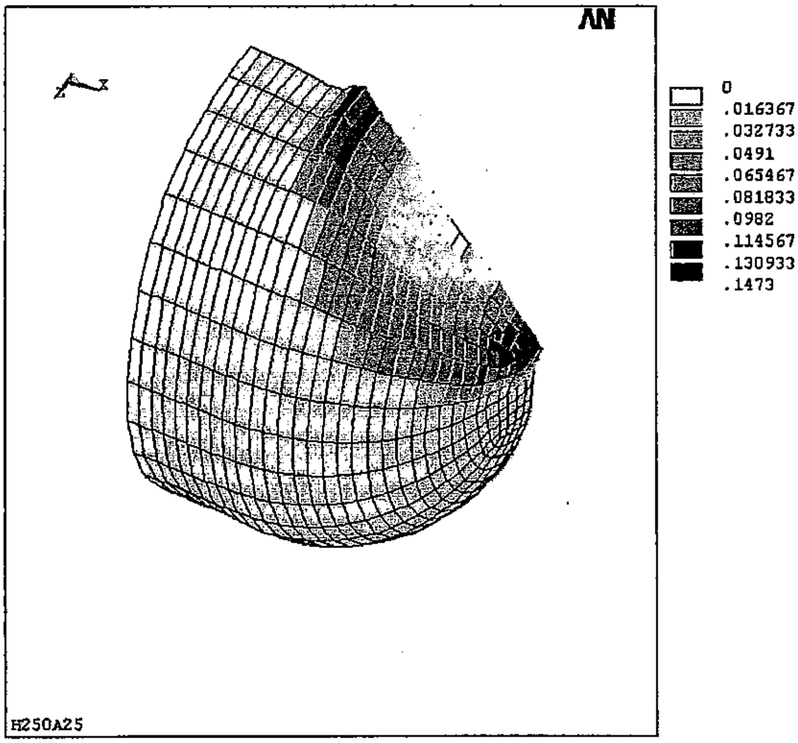

Figure 16: Effective Plastic Strain of 0.25 Inch Thick Hemispherical Head Impacting Rigid Wall at an Angle at 25 MPH

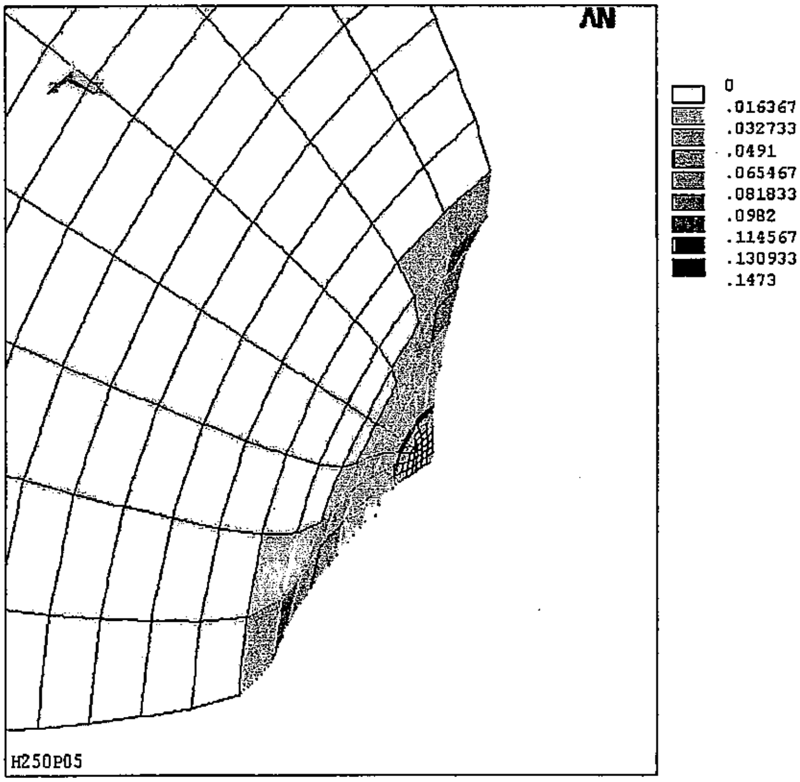

Figure 17: Effective Plastic Strain of 0.25 Inch Thick Hemispherical Head Impacting 6 Inch Post at 5 MPH

Variation in the distance between the primary and secondary heads appeared to have no significant effect on mitigating failure for the spacings that were evaluated (7, 11 and 15 inches).

Appendix B gives a summary of the effectiveness of the secondary head on raising the speed at which failure is initiated in the primary head.

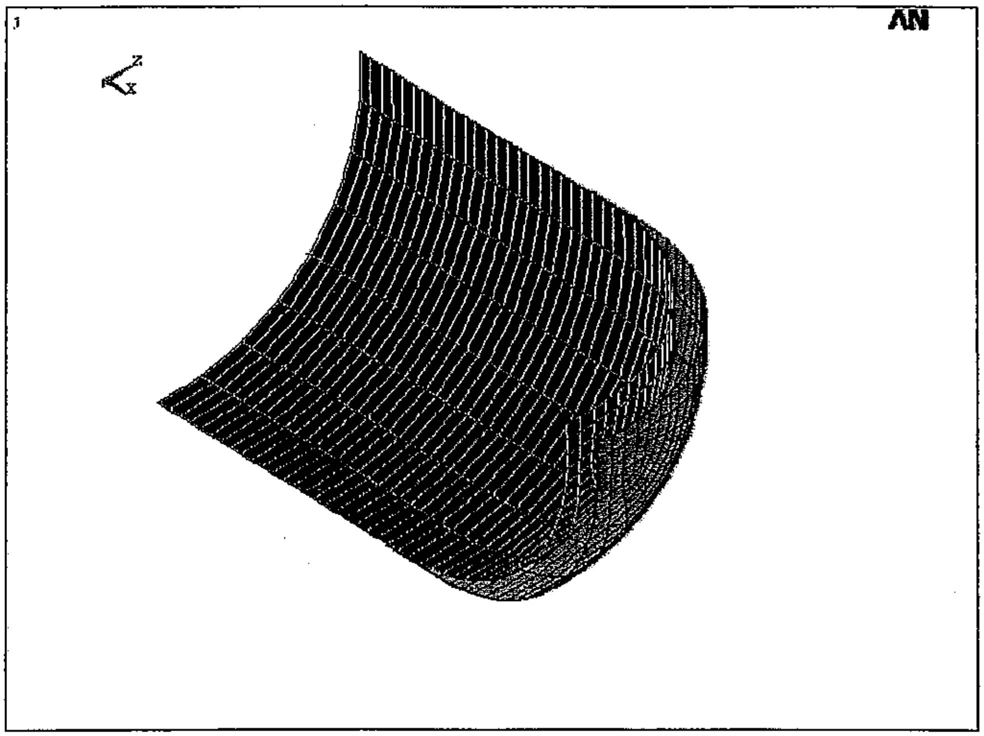

Figure 19: Finite Element Mesh of the Secondary Head

7.1 Impact into a Rigid Wall

The effect of a secondary head was analyzed for gaps of 7, 11 and 15 inches between the primary and secondary heads as shown on drawing PSI-98025-01, Revision C in Appendix C. The weld sizes shown on this drawing may need to be revised to ensure their adequacy; but this will not affect the energy-absorbing capability of the secondary head.

The secondary head failure was initiated at 15 MPH and primary head failure began at about the same speed, approximately 25 MPH, as without shielding. When shielding was placed 7 inches away from the primary head, the speed that causes initiation of the primary head failure is lower than that for the bare head. This may be related to the mesh density chosen or it could be related to the primary head impacting the buckled secondary head, which could cause increased local loadings.

The use of secondary head shielding, without energy-absorbing material, for impact into a rigid wall would appear to have less benefit than changing the hemispherical head to an ellipsoidal or torispherical shape.

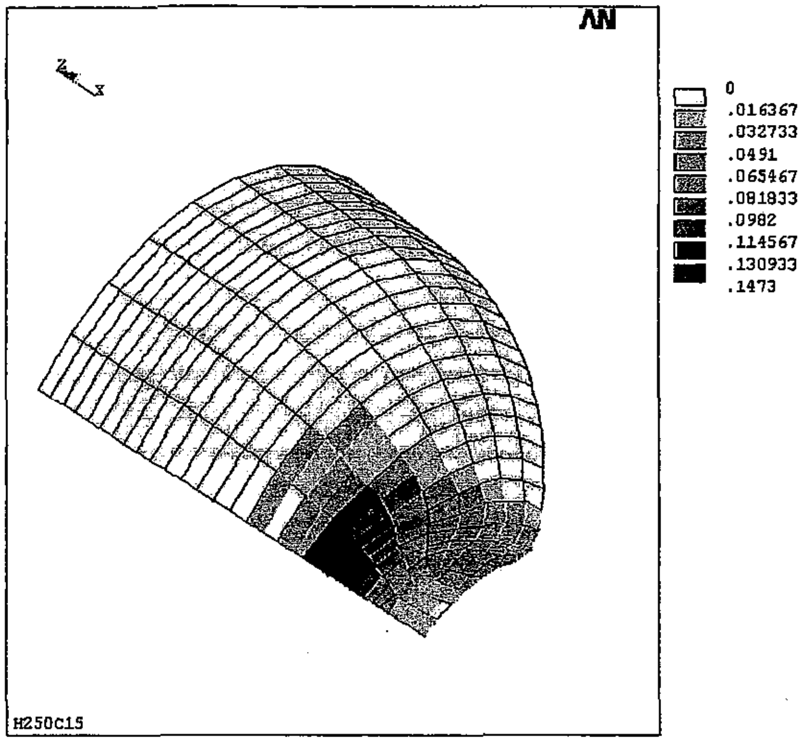

Figure 18: Effective Plastic Strain of 0.25 Inch Thick Hemispherical Head Impacting Column at 15 MPH

7 Task 04: Evaluate Secondary Head Shielding on MC-331 Cargo Tank Motor Vehicles

The four different impact scenarios used to evaluate the bare head designs were used to evaluate the effectiveness of a secondary head spaced at various distances from the primary head. The secondary head was added to the base design (0.250 inch thick hemispherical head) to compare the performance of the two heads in series with that of the base design alone. The finite element mesh for the secondary head is shown in Figure 19.

The failure strain criteria and the use of the eroding element capabilities of ANSYS/LS-DYNA allowed us to study the effectiveness of the secondary heads in a realistic manner. If elements that have exceeded the failure criteria are not eliminated from the solution, the primary head strains predicted in the analyses will be nonconservative, since the energy absorption capabilities of the secondary head are over-predicted.

In general, the secondary heads themselves failed at a lower impact speed than the bare head designs. This is most likely because of the presence of the pressurized fluid behind the primary head. For the two most severe scenarios considered (impact into a rigid wall and a rigid post) the addition of the secondary head alone provided no additional crashworthiness capability, (no higher speed at primary head failure). For the more realistic scenarios the speed at which failure begins was increased by almost 20 MPH for the angled impact and by 5 MPH for the column impact.

7.2 Impact into an Angled Wall

The greatest improvement in crashworthiness protection from the addition of a secondary head was for impacts into an angled wall. For gap sizes of 7 and 11 inches the primary head did not experience failure strains until a speed of 40 to 45 MPH. Figure 20 shows the results from analysis with the secondary head spaced at 7 inches. For the 15 inch spacing, failure strains in the primary head occurred between 45 and 50 MPH compared to a speed below 25 MPH for the bare heads. Considering that impact into a wall at an angle is a realistic accident scenario, the addition of a secondary head appears to have promise as a means to protect cargo tank motor vehicle heads.

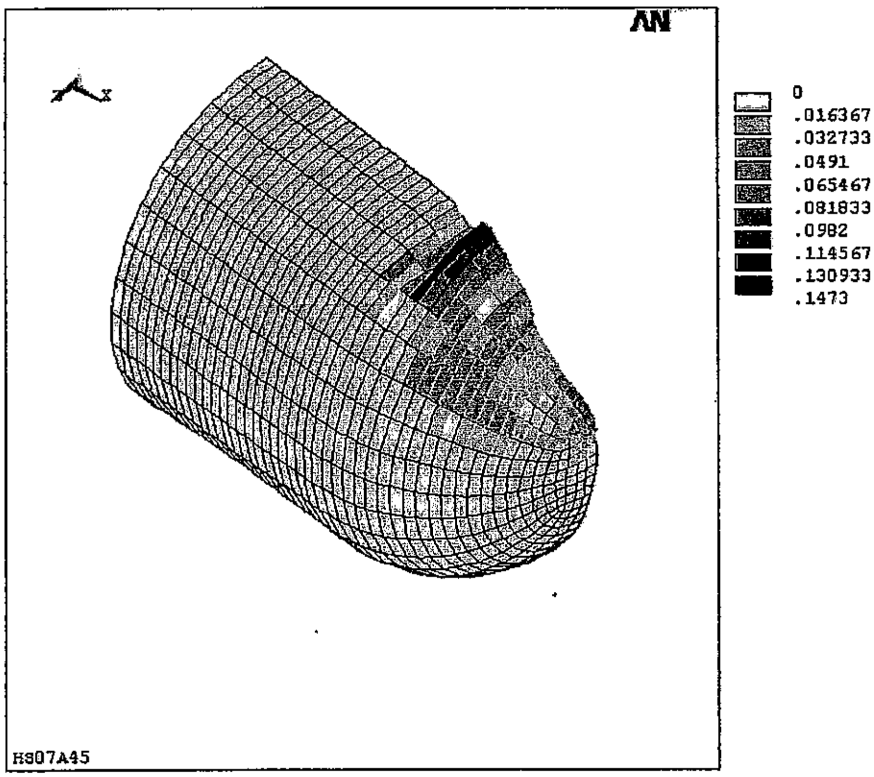

Figure 20: Effective Plastic Strain of 0.25 Inch Thick Primary Hemispherical Head With Secondary Head Spaced at 7 Inches, Impacting Rigid Wall at an Angle at 45 MPH

7.3 Penetration Impact

The amount of energy absorbed during the penetration of the secondary head appeared to be minimal, since for all the gap sizes considered the primary head was punctured below 5 MPH even with a secondary head.

7.4 Impact into a Column of Finite Strength

The use of a secondary head to mitigate failure when striking a column of finite strength increases the speed at which the primary head fails by approximately 5 MPH, which is about the same benefit gained by the increasing the head thickness. For all three gaps evaluated, the failure in the secondary head began below 10 MPH, in the primary head below 20 MPH, and the column failed above 30 MPH.

8 Task 05: Add Energy Absorbing Material to MC-331

Work performed under Task 05, considers the effectiveness of commercially available energy-absorbing material placed between the secondary head shield and the primary head to improve the resistance to penetration and failure of the MC-331 vessel heads.

Analyses were performed for the four accident scenarios with an energy-absorbing material filling the 7 inch gap between the primary and secondary head as shown on the drawing in Appendix C.

8.1 Description of Modeling of the Energy-Absorbing Material

The energy-absorbing material chosen for this study is a rigid polyurethane foam (LAST-A-FOAM® FR-3700) that is manufactured by General Plastics Manufacturing Company of Tacoma Washington. This material is a closed-cell CFC-free polyurethane foam available in densities from 3 to 40 lbs/cu ft that has been used by designers of nuclear transportation packages for crash applications. The last two digits of product numbers represent density, and we used LAST-A-FOAM® FR-3714.

For this study, it was decided to use the smallest thickness of foam capable of withstanding the impact speed at which failure was initiated in the base design (a bare 0.25 inch thick hemispherical head.). Preliminary calculations indicated that foam with a density of 14 lbs/cu ft at a thickness of 7 to 14 inches would be capable of withstanding a 25 MPH impact. The greater the thickness of the foam that can be used, the more deceleration that can be provided. If the foam density is too low, little or no deceleration will occur during impact until the foam bottoms out resulting in a minimal amount of crashworthiness protection. If the foam density is too high, the deflection of the foam will be limited resulting in low energy absorption by the foam and again a minimal amount of crashworthiness protection. For this task, only the 14 lbs/cu ft density foam was used. Future work should optimize the foam density and thickness to maximize the crash protection capability afforded by using crushable materials.

The energy-absorbing foam was modeled using ANSYS/LS-DYNA's low density foam material model. This material model requires an engineering stress-strain curve to characterize the nonlinear behavior associated with the foam. The stress-strain curve used in these analyses is shown in Appendix D.

In order to calibrate this material model Pressure Sciences, Inc. modeled the impact tests performed by General Plastics to create the stress-strain curve shown in Appendix D. The test consisted of a

680 pound pendulum mass striking a piece of foam having side dimensions of 2.677 and 2.675 inches and a thickness of 0.753 inch. The impact speed was 67.82 inches/second. The test results indicated a maximum foam stress of 1974 psi compared to the analytical stress of 2189 psi shown in Figure 21. Figure 21 shows the undeformed geometry and the crushed foam with an engineering strain of about 76%. Additional analyses were performed to match the unloading portion of the curve, with an ANSYS/LS-DYNA shape unloading factor of 6 and a viscous damping coefficient of 0.05. The resulting analytically-derived stress-strain curve is shown in Figure 22 and is seen to correlate well with the test-curve developed by General Plastics.

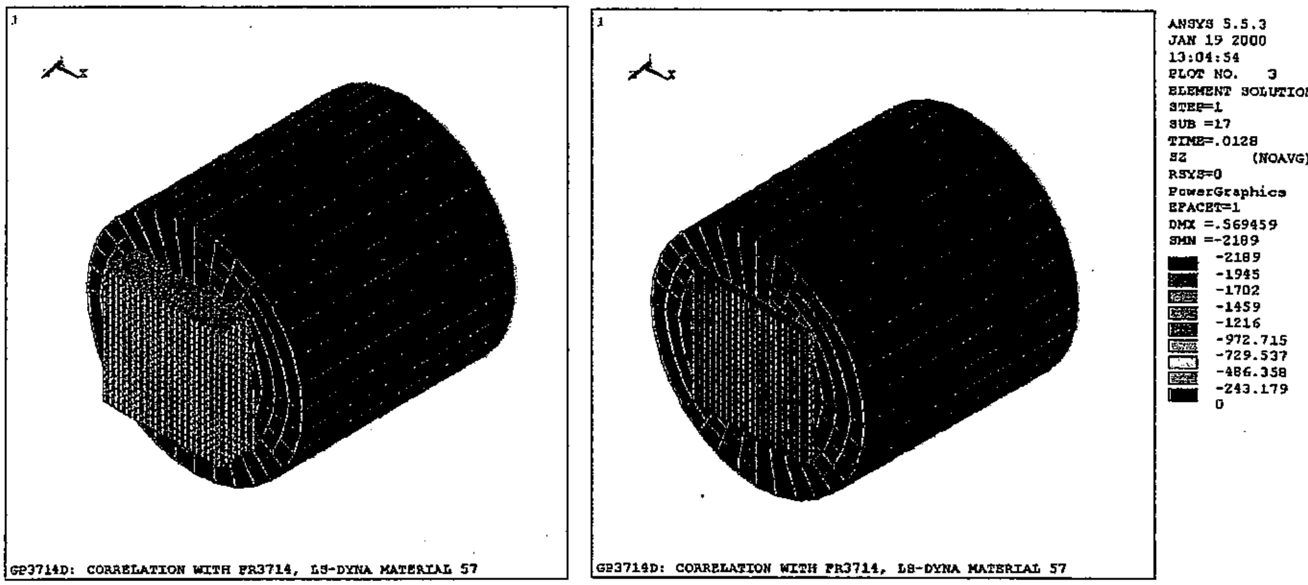

Figure 21: Calibration of Energy-Absorbing Foam

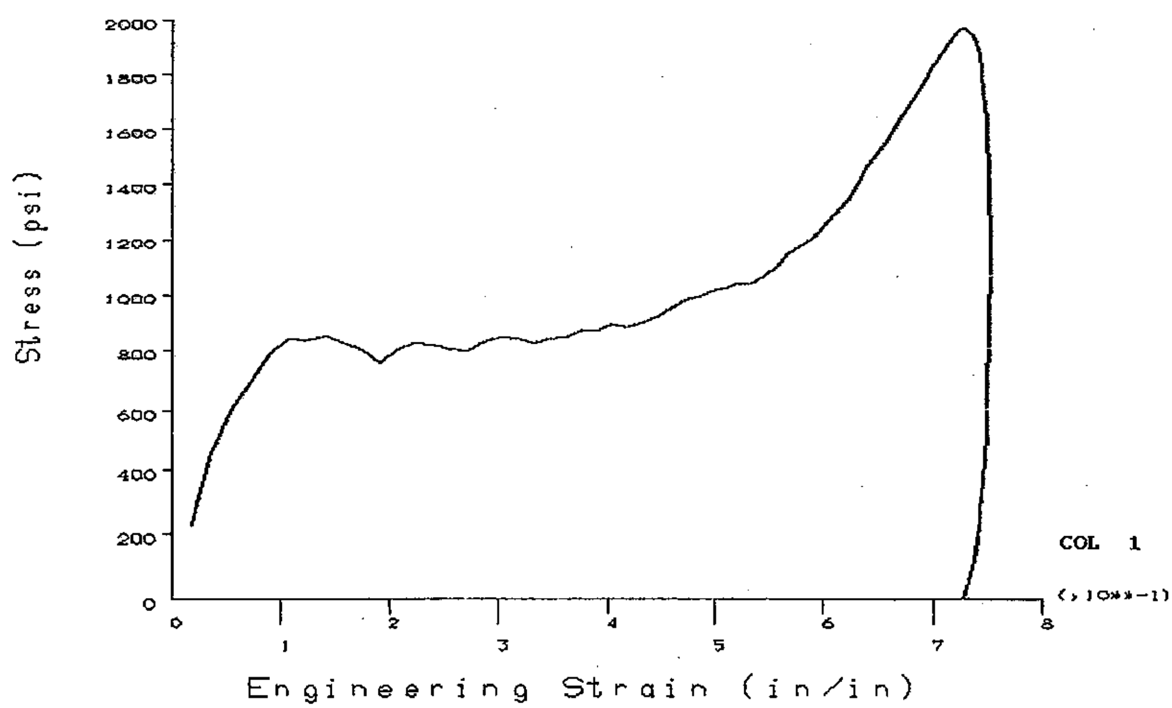

Figure 22: Analytical Stress-Strain Curve for Comparison with Appendix D

8.2 Conclusions Regarding the Addition of Energy-Absorbing Material

Appendix B gives a summary of the effects of including 7 inches of energy-absorbing material between the primary head and a secondary head. The inclusion of 7 inches of LAST-A-FOAM® FR-3714 increased the speed at which failure of the primary head was initiated by about 5 MPH. There is some evidence that the foam was bottoming out, which indicates that the foam density chosen for this study may have been too low. Increased thickness and density of the foam would be expected to further increase the speed at which failure of the primary head begins.

8.2.1 Frontal Impact into a Rigid Wall

The inclusion of 7 inches of LAST-A-FOAM®FR-3714 resulted in the primary head beginning to fail between 25 and 30 MPH. This is an improvement of 5 MPH over the bare head design and an improvement of 10 MPH over the design that incorporated a secondary head spaced at 7 inches. In addition to adding energy-absorbing capability, the foam would also tend to decrease any local effects associated with the primary head being struck by the buckled secondary head.

With the inclusion of the foam, the secondary head failed at a speed comparable to the bare primary head design failure speed.

In regions where the secondary head buckled, the engineering strain in the foam exceeded 70%. This indicates that the foam was bottoming out and that an increase in foam density foam and/or thickness should be considered.

In the ANSYS/LS-DYNA computer runs, some of the crushable foam elements became highly distorted and/or the elements became inverted such that their volume appeared to be negative to the computer program. This generally occurred when the secondary head elements began to fail. When a negative volume occurs in an element, the analysis becomes invalid and stops. The failure (erosion) of the secondary head elements (and the negative volume failures in the foam elements) occurred between 25 and 30 MPH. The maximum effective plastic strain in the primary head before the analysis became invalid was 14.4%. While this is slightly less than the failure criterion of 14.7%, a through review of the results indicates that had the analysis continued the primary head would have experienced strains of 14.7% at 30 MPH.

8.2.2 Angled Impact into a Rigid Wall

The addition of 7 inches of foam between the primary and secondary heads raised the speed at which failures in the primary and secondary heads began by about 5 MPH, as shown in Figure 23. For an angled impact, the area of impact is not as great as for a frontal impact; therefore, a smaller volume of the foam is effective in improving the crashworthiness of the heads.

Although negative volume failures occurred in the foam at 50 MPH, they occurred after the failure had been initiated in the primary head and after several secondary head elements had totally failed, as shown in Figure 24.

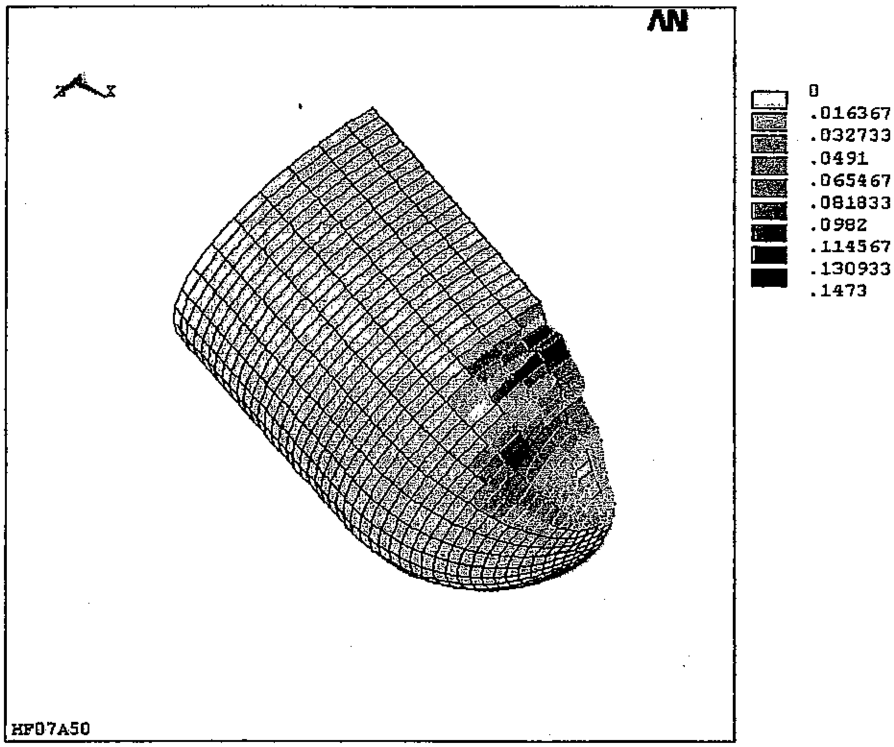

Figure 23: Effective Plastic Strain of 0.25 Inch Thick Primary Hemispherical Head With 7 Inches of Foam, Impacting Rigid Wall at an Angle at 50 MPH

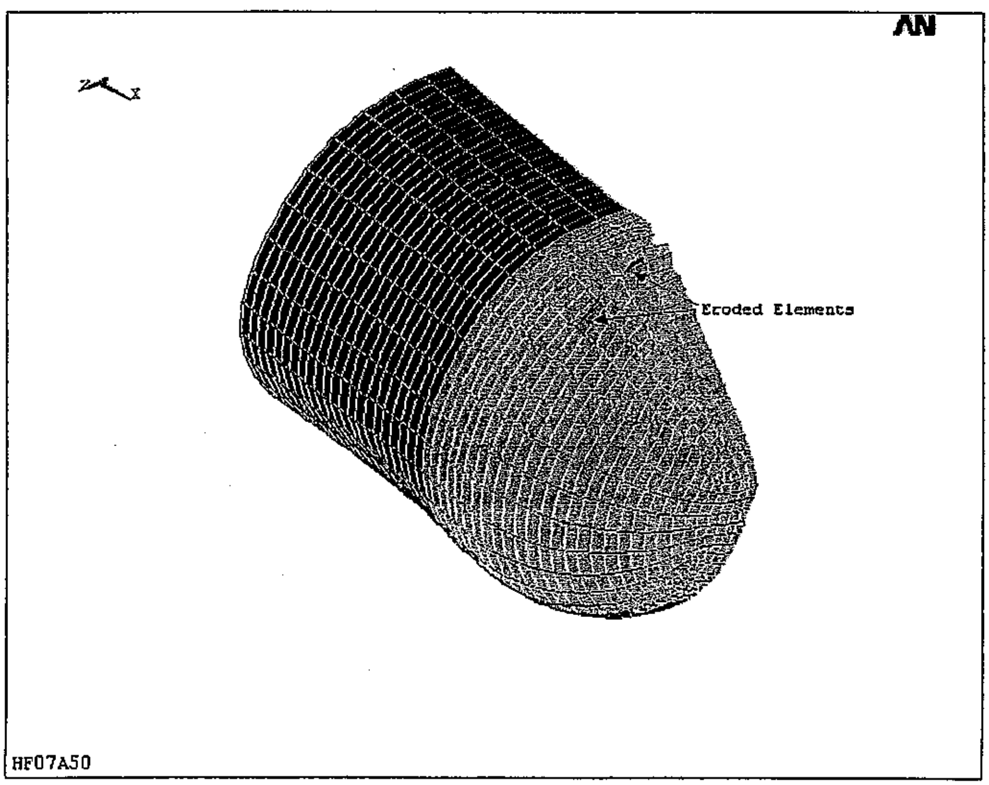

Figure 24: Secondary Head Eroded Elements with 7 Inches of Foam, Impacting Rigid Wall at an Angle at 50 MPH

This arrangement also allows for a greater tolerance on the secondary head dimensions, since the secondary head extension would allow some flexibility during assembly.

However, the inclusion of the chill band does limit the minimum distance between the primary and secondary head to about 7 inches.

Included in this conceptual design is a slotted hole (see detail A). This hole is intended to prevent pressure buildup between the secondary and primary heads, should the primary head develop a leak. This hole also provides a drainage outlet for condensation that may develop between the primary and secondary heads.

Foaming in place is the easiest way of including the energy-absorbing material between the primary and secondary heads. This also has the advantage of providing a perfect fit. The disadvantage with foaming in place is the cost associated with shipping the completed cargo tank vessel to the foam manufacturers' facility. The budgetary cost for the foaming work is approximately $4 to $6 per pound of material. There is approximately 2.5 cubic feet of foam for each inch of thickness. The density of the foam used in these analyses was 14 pounds per cubic foot. Therefore, the cost per inch of thickness of foam is approximately $140 to $210. For the 7 inch thick foam analyzed the cost per head is estimated to be about $1,500 not including any setup costs.

Other alternative methods include setting up a remote foaming facility or precasting the foam. A rough order of magnitude cost for developing a mold to precast the foam is $10,000. Additionally some tests to determine the amount of foam shrinkage would have to be performed during the development of the precasting mold.

A budgetary estimate for the cost of materials, manufacturing and installation for the chill-band and the secondary head is $5,000 - 6,000. Therefore, the budgetary unit cost of the foamed material plus the secondary head assembly will be $6,500 – $7,500 per cargo tank trailer.

10 Overall Conclusions

ANSYS/LS-DYNA can be used to model the complex interaction of steel, propane (in liquid and vapor states), foam, and roadway structures that occur when cargo tanker heads are involved in collisions. This was shown on a system level by correlations with the accident that occurred in White Plains, NY. The modeling of the fluid interaction was demonstrated by correlations with drop tests performed by the AAR and Lupker. The modeling of energy-absorbing foam material was validated by the close correlations obtained with the tests performed by General Plastics.

The use of effective plastic strain as a failure criterion was validated and ANSYS/LS-DYNA eroding elements were found to allow for evaluations of sacrificial secondary heads.

The incorporation of head shielding will improve the crashworthiness of the MC-331 cargo tanker, and result in fewer ruptures of the pressure boundary for the type of accidents most likely to occur. Protection against normal (perpendicular) impacts into a rigid flat surface or a rigid post is probably not a realistic goal. Protection against angled impacts into rigid surfaces or collisions with bridge

8.2.3 Penetration Impact

The addition of only 7 inches of foam did not substantially increase the ability of the secondary head to resist penetration. The foam where the 6 inch post impacted the head was highly strained and negative volume failure of the foam occurred almost immediately after the total failure of the secondary head.

The amount of effective plastic strain in the primary head at this point in the analysis was less than 1 percent. Additionally the speed of the tank had been reduced from 5 MPH to 1.1 MPH. This indicates that some protection of the primary head was gained by the addition of the 7 inches of foam. However, because of the negative volume failure of the foam elements, a quantitative assessment of the effectiveness of the foam on preventing a primary head failure due to a penetration impact cannot be made without refining the current techniques.

8.2.4 Impact into a Column of Finite Strength

The primary head began to fail between 20 and 25 MPH when the 7 inch gap between the secondary head and primary head was filled with crushable foam. This is an improvement of 10 MPH over the bare head design and an improvement of 5 MPH over the design that incorporated only a secondary head. With the inclusion of the foam, the speed at which the secondary head began to fail was increased by about 10 MPH.

The column also failed between 20 and 25 MPH. At 25 MPH the secondary head failed, then the column, and finally the primary head.

9 Produceability and Cost Considerations

The conceptual drawing shown in Appendix C was reviewed by representatives from General Plastics Manufacturing Company and Mr. Mike Pitts of Mississippi Tank Company. These reviews were intended to insure that the head shield shown and the crushable foam are feasible to produce.

For the analyses performed, the secondary head was assumed to be made of the same material as the primary head. However, since the secondary head is not part of the pressure boundary it does not need to be ASME Code material. Furthermore, additional analyses should be performed to determine if the ultimate and yield strength of the secondary head steel could be reduced without a reduction in the failure speed of the primary head.

The conceptual drawing includes a secondary head extension (item 5) and a chill band (item 6) in order to facilitate the use of non-ASME code material for the secondary head. These items enable welding of the secondary head to be done away from the ASME material required for the pressure boundary. Furthermore, with this arrangement it would be possible to hydrotest the ASME Code stamped components and add the secondary head afterwards. This would allow for greater ease of inspection of the primary head-to-shell weld during the hydrotest.

columns may be enhanced by placing energy absorbing material between the primary head and a secondary head.

Correlation with accidents that have previously occurred proved to be elusive except for the White Plains accident. The types of data (speed at impact, amount of deformation, descriptions of how the failures were initiated, etc.) that would be useful to mathematically simulate the accidents were generally not collected.

11 Recommendations

11.1 A cost/benefit analysis for the conceptual design presented in Appendix C should be prepared.

11.2 The amount and density of the foam used for this study was not optimized, which was evidenced by the foam bottoming out in several analyses. Future work will be required to optimize the amount and material characteristics of the crushable material placed between the primary and secondary heads.

11.3 Alternative materials, such as stainless steels that have much higher specified minimum elongation values, should be considered for the primary and secondary heads.

11.4 Discussions should be held with manufacturers regarding other possibilities to improve crashworthiness, such as changing the primary vessel diameter and lowering the center of gravity of the primary vessel.

11.5 If future post accident failure teams include a structural analyst to collect the necessary information, the ability to validate engineering analyses will be improved.

12 References

1. Selz, A. and Shaw, D.T., "Study of Enhanced Protection for MC 331 Cargo Tanks in Frontal Collisions," Pressure Sciences Inc., Report No. 96041-005, June 30, 1997 (NTIS Order # PB97-178693), 1997.

2. Phillips, E.A., and Olsen, "Final Phase 05 Report on Tank Car Head Study, "RPI-AAR Tank Car Safety Research Project," RA-05-17, 1972.

3. Jeong, D.Y.; Tang, Y.H.; Perlman, A.B.,"Evaluation of Semi-Empirical Analyses for Tank Car Puncture Velocity, Part I: Correlations with Experimental Data," Final Report (Draft), DOT-VNTSC-FRA-97-XX, Volpe National Transportation Systems Center, December 1997.

4. Jeong, D.Y., Tang, Y.H., Perlman, A.B.,"Evaluation of Semi-Empirical Analyses for Tank Car Puncture Velocity, Part II: Correlations with Engineering Analysis," Final Report (Draft), DOT-VNTSC-FRA-98-XX, Volpe National Transportation Systems Center, July 1998.

5. Lupker, H.A., "LPG Rail Tank Cars Under Head-On Collisions," International Journal of Impact Engineering, pages 359-376, 1990.

6. Metals Handbook Committee, *Metals Handbook*, 8th Edition, Vol. 1, "Properties and Selection of Metals", Metals Park, Ohio: American Society for Metals, p. 64, 1961.

7. "ANSYS/LS-DYNA, Theoretical Manual," ID Number 001121,ANSYS, Inc.: Canonsburg, PA, September 1998.

8. National Transportation Safety Board, "Propane Truck Collision with Bridge Column and Fire, White Plains, New York, July 27, 1994," NTSB/HAR-95/02, Washington, D.C., 1995.

9. Belytschko, T.; Ong, J.S.-J.; Liu, W.K.; and Kennedy, J.M. "Hourglass Control in Linear and Nonlinear Problems," Computer Methods in Applied Mechanics and Engineering, Vol. 43, pp. 251-276, 1984.

STATEMENT OF WORK

Investigate methods for reducing probability of fractures and/or penetration of the front head and adjacent structure of DOT Specification MC-331 cargo tank motor vehicles in highway accidents. This work will build upon the feasibility study and analytical tools developed under a contract (Procurement Request No. 957-6177) completed June 30, 1997.

1) Perform analyses to establish correlation between analytical models and damage resulting from actual accidents using investigative findings reported by the National Transportation Safety Board (NTSB).. As a minimum, NTSB reports and working documents, where available, on the following LPG semi-trailer accidents shall be reviewed and used as source material in this task:

12/23/88	Memphis, TN
01/20/92	Crawford, MS
07/27/94	White Plains, NY

This task will address damage both from impact with a flat plane and with a cylindrical column (e.g. a bridge support column) of finite mass and also from puncturing forces for the typical MC-33 1 cargo tanks involved in these accidents.

2) In considering the puncture mode, the contractor will coordinate the analytical programs employed in the feasibility study with analytical techniques developed by the Volpe National Transportation Systems Center in their work on similar failure modes of rail tank cars. Appropriate failure criteria will be established for puncture of single heads and for full or partial head shields.

3) Using results of Tasks 01 and 02, head shape and thickness will be varied to determine practical designs for bare (unprotected) heads having significantly better resistance to damage in these failure modes. This task includes coordination with one or more leading manufacturers of MC-331 cargo tank motor vehicles with respect to produceability and cost effects of candidate configurations.

4) Using the failure criteria established in Task 02., head shielding will be evaluated considering at least the following general arrangements:

a. a secondary head at various distances from the pressure-containing head, and

b. a secondary head with energy-absorbing material between it and the pressure-containing head.

Appendix A
Contract Statement of Work

Produceability and cost effects of head shields will be compared to data generated in Task 03; these findings will be coordinated with one or more leading manufacturers of MC-331 cargo tank motor vehicles.

5) Work performed will be documented in a final report. The report must conform to the latest issuance of ANSI Standard Z39.18 "Scientific and Technical Reports - Organization, Preparation and Production." Submit six original quality copies of the final report to the COTR, along with a copy of the report on a diskette in Word Perfect 6.1 format.

A completed Standard Form SF 298, "Report Documentation Page" will be submitted by the contractor to the COTR to assist in transmittal of the report by the government to the National Technical Information Service (NTIS). Standard Form 298 is available from the COTR. Instructions for its completion are printed on the back of the form.

Appendix B
Summary of Design Alternative Runs

Angled Runs: Speed (MPH) to Failure

		Primary	Secondary	
Hemispherical Head, t=0.250"	Bare	25	NA	
	7" Shield	45	30	
	11" Shield	45	30	
	15" Shield	50	30	
	7" Foam	50	35	
Hemispherical Head, t=0.378"	Bare	25	NA	
Ellipsoidal Head, t=0.363"	Bare	25	NA	The failure occurred in the shell, not the head.
Torispherical Head, t=0.757"	Bare	15	NA	The failure occurred near the knuckle radius.

Column Impact Runs: Speed (MPH) to Failure

		Primary	Secondary	
Hemispherical Head t=0.250"	Bare	15	NA	Column failed between 25 and 30 MPH
	7" Shield	20	10	Column failed above 30 MPH
	11" Shield	20	10	Column failed above 30 MPH
	15" Shield	20	10	Column failed above 30 MPH
	7" Foam	25	20	Column failed between 20 and 25 MPH
Hemispherical Head, t=0.378"	Bare	15	NA	Column failed between 15 and 20 MPH
Ellipsoidal Head, t=0.363"	Bare	20	NA	Column failed above 30 MPH
Torispherical Head, t=0.757"	Bare	25	NA	Column failed between 20 and 25 MPH

Rigid Impact Runs: Speed (MPH) to Failure

		Primary	Secondary	
Hemispherical Head t=0.250"	Bare	25	NA	Twice mesh density indicated failure at 15 MPH (2 elements)
	7" Shield	20	15	Secondary head failure may have "punctured" primary head.
	11" Shield	25	15	
	15" Shield	25	15	
	7" Foam	30	25	
Hemispherical Head, t=0.378"	Bare	15	NA	Bending thicker plates a given amount produces higher strains. Twice mesh density indicated failure at 15 MPH (3 elements) Twice mesh density strains still greater than t=0.250" run.
Ellipsoidal Head, t=0.363"	Bare	25	NA	15 MPH, 2x-mesh density indicates 8% higher strains, no failure. 20 MPH, 2x-mesh density indicates 27% higher strains, no failure 25 MPH, 2x-mesh density indicates failure.
Torispherical Head, t=0.757"	Bare	30	NA	

Penetration Runs: Speed (MPH) to Failure

		Primary	Secondary	
Hemispherical Head t=0.250"	Bare	5	NA	
	7" Shield	5	5	
	11" Shield	5	5	
	15" Shield	5	5	
	7" Foam	Invalid	5	Speed had reduced to 1.1 MPH before analysis was aborted due to negative volume foam elements.
Hemispherical Head, t=0.378"	Bare	10	NA	
Ellipsoidal Head, t=0.363"	Bare	10	NA	At 5 MPH, the fluid mesh became unstable (negative volume elements) before a judgment could be made about the shell. Speed had been reduced to 3.7 MPH before the 5 MPH run aborted. At 10 MPH, the shell failed before the analysis aborted due to negative volume fluid elements.
Torispherical Head, t=0.757"	Bare	5	NA	

Appendix C
Conceptual Head Shielding Drawing
PSI-98025-01, Rev. C

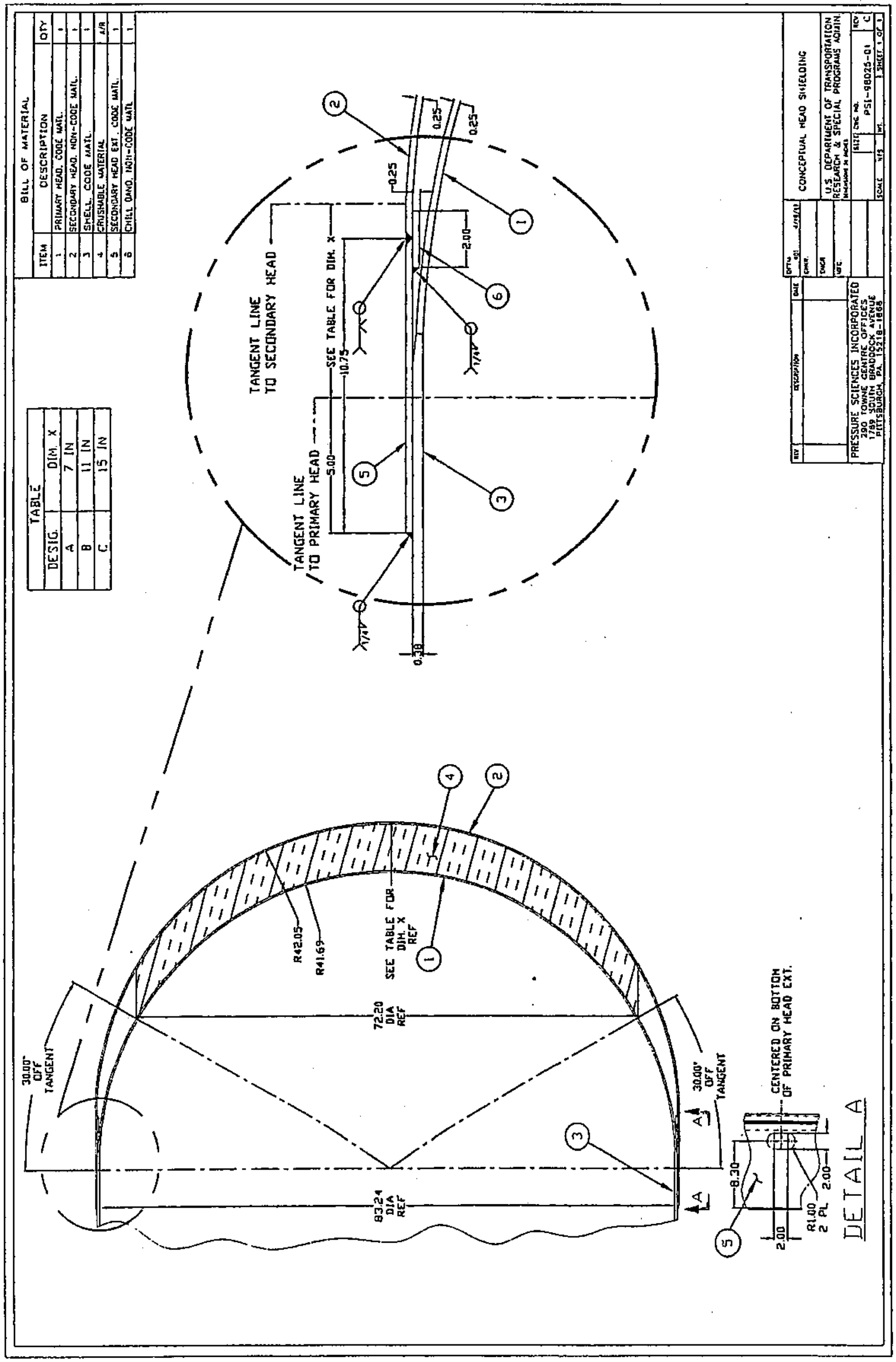
BILL OF MATERIAL
ITEM DESCRIPTION QTY
1 PRIMARY HEAD, CODE MAT'L. 1
2 SECONDARY HEAD, NON-CODE MAT'L. 1
3 SHELL, CODE MAT'L. 1
4 CRUSHABLE MATERIAL A/R
5 SECONDARY HEAD EXT., CODE MAT'L. 1
6 CHILL BAND, NON-CODE MAT'L. 1
TABLE
DESIG. DIM. X
A 7 IN
B 11 IN
C 15 IN
TANGENT LINE TO SECONDARY HEAD
TANGENT LINE TO PRIMARY HEAD
SEE TABLE FOR DIM. X
10.75
5.00
2.00
0.25
0.38
1/4
R42.05
R41.69
SEE TABLE FOR DIM. X REF
72.20 DIA REF
83.24 DIA REF
30.00° OFF TANGENT
CENTERED ON BOTTOM OF PRIMARY HEAD EXT.
8.30
R1.00 2 PL
DETAIL A
CONCEPTUAL HEAD SHIELDING
U.S. DEPARTMENT OF TRANSPORTATION RESEARCH & SPECIAL PROGRAMS ADMIN.
PRESSURE SCIENCES INCORPORATED
290 TOWNE CENTRE OFFICES
1789 SOUTH BRADDOCK AVENUE
PITTSBURGH, PA. 15218-1868
PSI-98025-01
C

Appendix D
Stress-Strain Curve Used to Model Crushable Foam

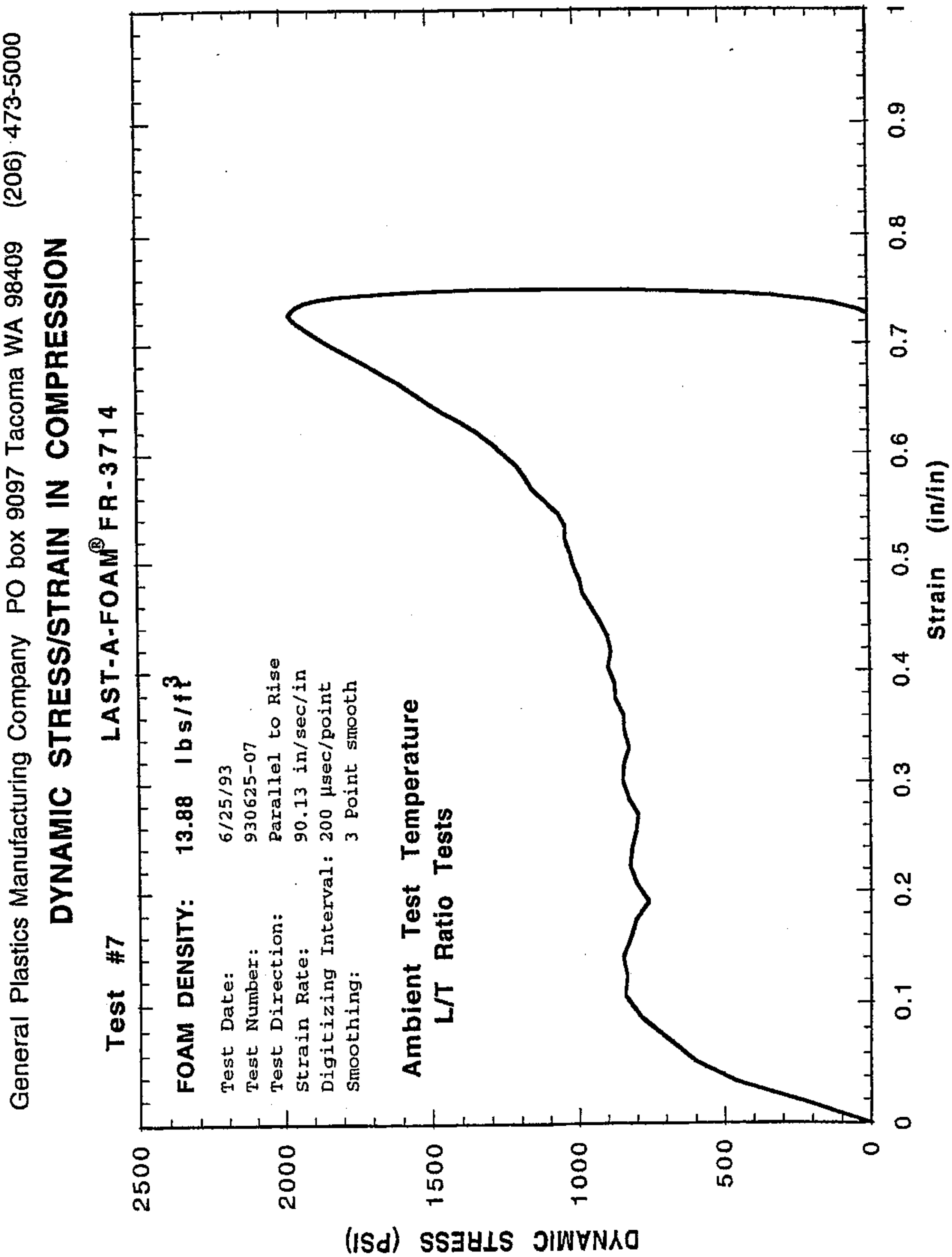
General Plastics Manufacturing Company PO box 9097 Tacoma WA 98409 (206) 473-5000
DYNAMIC STRESS/STRAIN IN COMPRESSION
Test #7
LAST-A-FOAM® FR-3714
FOAM DENSITY: 13.88 lbs/ft3
Test Date: 6/25/93
Test Number: 930625-07
Test Direction: Parallel to Rise
Strain Rate: 90.13 in/sec/in
Digitizing Interval: 200 µsec/point
Smoothing: 3 Point smooth
Ambient Test Temperature
L/T Ratio Tests
DYNAMIC STRESS (PSI)
2500
2000
1500
1000
500
0
Strain (in/in)
0
0.1
0.2
0.3
0.4
0.5
0.6
0.7
0.8
0.9
1